



**AFRL-RH-FS-TR-2014-0035**

**MATILDA: A Military Laser Range Safety  
Tool Based on Probabilistic Risk Assessment  
(PRA) Techniques**



Paul Kennedy  
**711th Human Performance Wing  
Human Effectiveness Directorate  
Directed Energy Bioeffects Division  
Optical Radiation Bioeffects Branch**

Brian K. Flemming  
David G. Devoy  
**SELEX ES Ltd.**

Daniel F. Huantes  
**TASC, Inc.**

Matthew D. Flowers  
**UK Military Laser Safety Committee**

**August 2014**

**Interim Report for January 2013 to July 2014**

**Distribution A: Approved for public  
release; distribution unlimited. PA  
Case No: TSRL-PA-2014-0021**

**STINFO COPY**

**Air Force Research Laboratory  
711th Human Performance Wing  
Human Effectiveness Directorate  
Bioeffects Division  
Optical Radiation Bioeffects Branch  
Fort Sam Houston, Texas 78234**

## NOTICE AND SIGNATURE PAGE

Using Government drawings, specifications, or other data included in this document for any purpose other than Government procurement does not in any way obligate the U.S. Government. The fact that the Government formulated or supplied the drawings, specifications, or other data does not license the holder or any other person or corporation; or convey any rights or permission to manufacture, use, or sell any patented invention that may relate to them.

This report was cleared for public release by the 88<sup>th</sup> ABW Public Affairs Office and is available to the general public, including foreign nationals. Copies may be obtained from the Defense Technical Information Center (DTIC) (<http://www.dtic.mil>).

MATILDA: A Military Laser Range Safety Tool Based on Probabilistic Risk Assessment (PRA) Techniques

(AFRL-RH-FS-TR- 2014 - 0035 ) has been reviewed and is approved for publication in accordance with assigned distribution statement.

KENNEDY.PAUL.K.1231446318  Digitally signed by KENNEDY.PAUL.K.1231446318  
DN: c=US, o=U.S. Government, ou=DoD, ou=PKI,  
ou=USAF, cn=KENNEDY.PAUL.K.1231446318  
Date: 2014.07.31 12:21:06 -05'00'

---

PAUL KENNEDY, Ph.D.  
Work Unit Manager  
Optical Radiation Bioeffects Branch

POLHAMUS.GARRETT.D.1175839484  Digitally signed by POLHAMUS.GARRETT.D.1175839484  
DN: c=US, o=U.S. Government, ou=DoD, ou=PKI,  
ou=USAF, cn=POLHAMUS.GARRETT.D.1175839484  
Date: 2014.10.01 08:27:00 -05'00'

---

GARRETT D. POLHAMUS, DR-IV, DAF  
Chief, Bioeffects Division  
Human Effectiveness Directorate  
711th Human Performance Wing  
Air Force Research Laboratory

This report is published in the interest of scientific and technical information exchange, and its publication does not constitute the Government's approval or disapproval of its ideas or findings.

<b>REPORT DOCUMENTATION PAGE</b>			<i>Form Approved</i> <i>OMB No. 0704-0188</i>		
Public reporting burden for this collection of information is estimated to average 1 hour per response, including the time for reviewing instructions, searching existing data sources, gathering and maintaining the data needed, and completing and reviewing this collection of information. Send comments regarding this burden estimate or any other aspect of this collection of information, including suggestions for reducing this burden to Department of Defense, Washington Headquarters Services, Directorate for Information Operations and Reports (0704-0188), 1215 Jefferson Davis Highway, Suite 1204, Arlington, VA 22202-4302. Respondents should be aware that notwithstanding any other provision of law, no person shall be subject to any penalty for failing to comply with a collection of information if it does not display a currently valid OMB control number. <b>PLEASE DO NOT RETURN YOUR FORM TO THE ABOVE ADDRESS.</b>					
<b>1. REPORT DATE (DD-MM-YYYY)</b> 01-08-2014	<b>2. REPORT TYPE</b> Interim Technical Report		<b>3. DATES COVERED (From - To)</b> January 2013- July 2014		
<b>4. TITLE AND SUBTITLE</b> MATILDA: A Military Laser Range Safety Tool Based on Probabilistic Risk Assessment (PRA) Techniques			<b>5a. CONTRACT NUMBER</b> FA8650-14-D-6519		
			<b>5b. GRANT NUMBER</b>		
			<b>5c. PROGRAM ELEMENT NUMBER</b> 0603231F		
<b>6. AUTHOR(S)</b> Paul K. Kennedy, Brian K. Flemming, David G. Devoy, Daniel F. Huantes, Matthew D. Flowers			<b>5d. PROJECT NUMBER</b> 7757		
			<b>5e. TASK NUMBER</b> HD		
			<b>5f. WORK UNIT NUMBER</b> 02		
<b>7. PERFORMING ORGANIZATION NAME(S) AND ADDRESS(ES)</b> Air Force Research Laboratory 711th Human Performance Wing Human Effectiveness Directorate Bioeffects Division Optical Radiation Bioeffects Branch Fort Sam Houston, Texas 78234			<b>8. PERFORMING ORGANIZATION REPORT</b> TASC, Inc. 4141 Petroleum Rd Fort Sam Houston, Texas 78234		
<b>9. SPONSORING / MONITORING AGENCY NAME(S) AND ADDRESS(ES)</b> Air Force Research Laboratory 711th Human Performance Wing Human Effectiveness Directorate Bioeffects Division Optical Radiation Bioeffects Branch Fort Sam Houston, Texas 78234			<b>10. SPONSOR/MONITOR'S ACRONYM(S)</b> 711 HPW/RHDO		
			<b>11. SPONSOR/MONITOR'S REPORT NUMBER(S)</b> AFRL-RH-FS-TR-2014-0035		
<b>12. DISTRIBUTION / AVAILABILITY STATEMENT</b> Distribution A: Approved for public release; distribution unlimited. PA Case No: TSRL-PA-2014-0021					
<b>13. SUPPLEMENTARY NOTES</b>					
<b>14. ABSTRACT</b> Recently, the use of Probabilistic Risk Assessment (PRA) techniques to perform laser safety and hazard analysis for high output lasers in outdoor environments has become an increasingly accepted alternative to standard risk analysis methods, based on Maximum Permissible Exposure (MPE) limits. Over the past ten years, the United Kingdom (UK) Ministry of Defence (MoD) and the United States (US) Air Force Research Laboratory (AFRL) have collaborated to develop a jointly-owned, PRA-based, laser Range safety tool, the Military Advanced Technology Integrated Laser hazard Assessment (MATILDA) system. The UK MoD has been developing PRA-based laser hazard analysis models for nearly four decades, and using them to assess laser irradiation risks to unprotected persons from laser test and training operations on UK military Ranges. The Air Force Research Laboratory wishes to develop PRA-based hazard analysis models for outdoor high energy laser applications, and began the collaboration to leverage the PRA modelling expertise of the UK. Initial MATILDA code development was based on the PRA "partition" model developed to perform Range safety clearances for the UK Thermal Imaging Airborne Laser Designator (TIALD) system. MATILDA is the first military software tool to contain a complete end-to-end laser PRA model, crafted for Range applications, and with generalized terrain modelling. In the future it will provide a starting point for development of more advanced laser PRA models and tools.					
<b>15. SUBJECT TERMS</b> Laser safety, range safety, laser hazard analysis, probabilistic risk assessment					
<b>16. SECURITY CLASSIFICATION OF:</b> Unclassified			<b>17. LIMITATION OF ABSTRACT</b>  U	<b>18. NUMBER OF PAGES</b>  51	<b>19a. NAME OF RESPONSIBLE PERSON</b> Paul Kennedy
<b>a. REPORT</b> U	<b>b. ABSTRACT</b> U	<b>c. THIS PAGE</b> U			<b>19b. TELEPHONE NUMBER (include area code)</b> NA

Standard Form 298 (Rev. 8-98)  
Prescribed by ANSI Std. Z39.18

**This Page Intentionally Left Blank**

# TABLE OF CONTENTS

TABLE OF CONTENTS .....	iii
TABLE OF FIGURES .....	iv
LIST OF TABLES .....	iv
ABSTRACT .....	1
1 INTRODUCTION .....	1
2 UK LASER PRA MODEL .....	3
2.1 UK Need for a PRA-Based Approach .....	3
2.2 A Risk-Based Approach to Laser Hazard Assessment .....	8
2.3 Probabilistic Laser Pointing Error Modelling .....	10
2.4 Probabilistic Ocular Damage Modelling .....	12
2.5 UK Expectation Model .....	13
2.6 UK Partition Model .....	16
2.7 Computational Model .....	17
3 THE MATILDA TOOL .....	19
3.1 Genesis of MATILDA .....	19
3.2 MATILDA Development and Testing .....	20
3.3 MATILDA Inputs, Set-Up Procedures, and Sample Case .....	21
3.4 RBPROG Analysis .....	26
3.5 CALCZONE Analysis and Attack Track Definition .....	32
3.6 CALCFAULT Analysis .....	39
4 DISCUSSION .....	44
5 CONCLUSIONS .....	45
6 REFERENCES .....	47

## LIST OF FIGURES

Figure 1: Laser Safety Risk Management Process .....	5
Figure 2: The “PE-PI-POD” Catastrophic Chain of Events Model .....	7
Figure 3: Risk Quadrant for an Adverse Event .....	8
Figure 4: The Selex ES “Onion-Skin” Fault/Failure Condition Model .....	11
Figure 5: Fault-Free Overshoot & Undershoot .....	18
Figure 6: MATILDA Coordinate Transformations .....	22
Figure 7: Geocentric and MICS Coordinates .....	23
Figure 8: Terrain Profile “Web” .....	24
Figure 9: The MATILDA Pro Primary Geographic Inputs .....	26
Figure 10: Star-Shaped Condition .....	27
Figure 11: Points of Closest Approach Condition .....	28
Figure 12: Terrain Profile Condition .....	29
Figure 13: Urban Area Condition .....	30
Figure 14: Small Increment Condition .....	30
Figure 15: Undershoot/Overshoot Condition .....	31
Figure 16: RBPROG Analysis Result: CRA with Additional Boundary Points .....	32
Figure 17: Spherical Earth Target – Range Boundary Overshoot Geometry .....	34
Figure 18: Spherical Earth Target – Range Boundary Undershoot Geometry .....	34
Figure 19: Geocentric Overshoot Geometry and Parameters .....	35
Figure 20: Terrain Undershoot Problem .....	37
Figure 21: MATILDA Generated Fault-Free Laser Firing Zones .....	38
Figure 22: Fault-Free Attack Track Check .....	39
Figure 23: Comparison of EMOVL Values to the EMOVLMAX Criterion .....	43
Figure 24: Comparison of a PRA-Based Laser Hazard Area Trace with a Deterministic Ocular Hazard Zone .....	44

## LIST OF TABLES

Table 1: Input Parameters for the Hypothetical Airborne Laser Designator .....	25
--	----

## NOMENCLATURE

Range	a geographic area used for military test and training
range	a distance, as in range-to-target
$P_E$	probability of laser energy being fired in an inappropriate direction outside the Controlled Range Area (CRA)
$P_I$	probability of an unprotected observer being irradiated by laser energy fired outside the CRA
$P_{OD}$	probability of the irradiated observer sustaining an ocular injury
$P_F$	probability of a laser system fault or failure during a laser firing maneuver
$E_{MOVL}$	expected number of observers who sustain a Minimum Ophthalmoscopically Visible Lesion (MOVL) during a laser firing maneuver
$E_{MOVLMAX}$	maximum acceptable value of $E_{MOVL}$
$e_{MOVL}$	expected number of observers who sustain a MOVL for a single laser pulse, emitted during a laser firing maneuver
$E_{CONMAX}$	maximum acceptable value of $E_{MOVL}$ for a laser firing maneuver where laser energy is inadvertently misdirected outside the CRA
$P_{MOVLMAX}$	maximum acceptable value of the probability that an irradiated individual will sustain a MOVL
MKS	Meters, Kilograms, Seconds: a system of physical units

**This Page Intentionally Left Blank**

## **ABSTRACT**

Recently, the use of Probabilistic Risk Assessment (PRA) techniques to perform laser safety and hazard analysis for high output lasers in outdoor environments has become an increasingly accepted alternative to standard risk analysis methods, based on Maximum Permissible Exposure (MPE) limits. Over the past ten years, the United Kingdom (UK) Ministry of Defence (MoD) and the United States (US) Air Force Research Laboratory (AFRL) have collaborated to develop a jointly-owned, PRA-based, laser Range safety tool, the Military Advanced Technology Integrated Laser hazard Assessment (MATILDA) system. The UK MoD has been developing PRA-based laser hazard analysis models for nearly four decades, and using them to assess laser irradiation risks to unprotected persons from laser test and training operations on UK military Ranges. The Air Force Research Laboratory wishes to develop PRA-based hazard analysis models for outdoor high energy laser applications, and began the collaboration to leverage the PRA modelling expertise of the UK. Initial MATILDA code development was based on the PRA “partition” model developed to perform Range safety clearances for the UK Thermal Imaging Airborne Laser Designator (TIALD) system. MATILDA is the first military software tool to contain a complete end-to-end laser PRA model, crafted for Range applications, and with generalized terrain modelling. In the future it will provide a starting point for development of more advanced laser PRA models and tools.

## **1 INTRODUCTION**

Recently, the use of Probabilistic Risk Assessment (PRA) techniques [1,2] to perform laser safety and hazard analysis for high output lasers in outdoor environments [3-6] has become an increasingly accepted alternative to standard risk analysis methods [7], based on Maximum Permissible Exposure (MPE) limits [8,9]. Over the past ten years, the United Kingdom (UK) Ministry of Defence (MoD) and the United States (US) Air Force Research Laboratory (AFRL) have collaborated to develop a jointly-owned, PRA-based, laser Range safety tool, the Military Advanced Technology Integrated Laser hazard Assessment (MATILDA) system [10-14]. This collaboration has been covered, sequentially, by two US-UK Project Arrangements (PAs): No. DOD-MOD-AF-06-0004 (2007-2012) and No. DOD-MOD-AF-12-0004 (2012-2017).

The move towards PRA, by some laser safety experts and organizations, has been driven by the limitations of standard, or MPE-based, risk analysis. In a standard risk analysis, exposures are simply characterized as safe or unsafe based on comparison to the MPE; no quantitative estimate of risk is provided. Standard risk analysis also implicitly assumes that risk can be completely mitigated [6], giving a “sure-safe,” or zero risk, condition as a final result. In controlled indoor environments, such as factories or labs, this may be true, or nearly true. In uncontrolled outdoor environments, such as military test Ranges or combat operations, a true zero risk condition is unachievable. Thus, a method giving a quantitative estimate of risk (PRA) is preferable.

PRA-based laser hazard analysis offers a number of advantages over standard risk analysis methods. First, it provides a quantified assessment of human risk (probability of injury) as a function of location. Second, it captures the probabilities and consequences of human error and

laser fault/failure conditions, factors which are critical to valid hazard assessments for military laser operations in uncontrolled outdoor environments. Third, and most importantly, PRA analysis does not assume, or require, a zero risk condition as a final result. Instead, it compares the quantified risk against a maximum acceptable (non-zero) risk value. This produces less restrictive Range clearances, while still maintaining acceptable safety levels for Range personnel and members of the public. This last advantage is critical for the UK, where the small size of UK Ranges and the possibility that laser beams might escape Range boundaries make a zero risk condition for Range testing unacceptably restrictive.

The UK MoD has been developing PRA-based laser hazard analysis models for nearly four decades, and using them to assess laser irradiation risks to unprotected persons from laser test and training operations on UK military Ranges. Over that time, PRA-based Range clearance techniques have ensured the safe operation of airborne and ground-based military laser rangefinders and target designators during development trials and operational training exercises. Prior to the US-UK collaboration, however, the MoD had not allocated the resources to create an expert software tool like MATILDA, which performs a complete end-to-end PRA hazard analysis for airborne laser Range applications, with generalized terrain modelling.

Beginning in 1998, with AFRL safety support to the Airborne Laser (ABL) and Advanced Tactical Laser (ATL) programs, the United States Air Force (USAF) had the goal of developing PRA-based hazard analysis models for outdoor high energy laser (HEL) applications. Very long HEL hazard distances, combined with the uncertainties inherent in outdoor operations, make zero risk unachievable in HEL Range tests. Thus, in assessing the potential risks posed by HEL operations, a shift to probabilistic analysis is preferable. The US began the collaboration described in this paper in order to leverage the PRA modelling expertise of the UK, with an eye to future development of an HEL PRA tool. Development of US HEL PRA tools is in fact underway at this time, but it has not been completed and will not be documented here. The purpose of this report is to document the development and capabilities of Version-1.6.2 of the MATILDA tool, which is currently valid only for direct beam hazards, created by low-to-moderate power airborne laser designators, operating at 1064 nm, and firing at stationary targets on military ranges.

In the development of MATILDA, UK PRA modelling experience was combined with AFRL expertise in development of complex software tools for laser hazard analysis and laser Range safety. Initial MATILDA code development (2007–2012) was based on the PRA “partition” model developed to perform Range safety clearances for the UK Thermal Imaging Airborne Laser Designator (TIALD) system. The TIALD model “fault-free” laser hazard analysis is geometrically similar to the standard risk analysis methods currently used for laser safety clearances on US Ranges [7]. However, the TIALD model contains an additional probabilistic hazard analysis component, which assesses probability of injury to an unprotected person in the event of a fault or failure in the laser directional control system. The “UK Laser PRA Model,” described in Section 2, refers to the TIALD model, as implemented in MATILDA.

The MATILDA system is a new software tool based on open-source Geographic Information System (GIS) technology that integrates relevant laser system performance parameters with environmental data appropriate to the Range location where the system is being operated. The

first five-year US-UK collaboration (2007–2012) was successfully completed by the release of Version-1.6.2 of MATILDA, which is documented in this report. The second five-year collaboration (2012–2017) is currently underway, with the goal of producing an updated version of MATILDA, with enhanced capabilities. MATILDA is the first military software tool to contain a complete end-to-end laser PRA model, crafted for Range applications, and with generalized terrain modelling. In the future it will provide a starting point for development of more advanced laser PRA models and tools.

## **2 UK LASER PRA MODEL**

### **2.1 UK Need for a PRA-Based Approach**

The primary hazard associated with the use of low-to-moderate power lasers on military Ranges is potential injury to exposed tissue, in particular the eye. While protective measures can be applied for persons within the Controlled Range Area (CRA), the main concern – particularly in the case of airborne laser target designators and rangefinders – is avoidance of possible ocular injury to unprotected members of the general public, should laser energy escape the confines of the Range. Traditionally, the ocular hazards associated with a laser’s output have been assessed in terms of the Maximum Permissible Exposure, from which a corresponding Nominal Ocular Hazard Distance (NOHD) is determined [8,9]. The NOHD represents a safe viewing distance at which an observer can be exposed to the laser energy over a given period of time without risk of injury to the eye. Typical exposure periods for military laser systems can vary from the order of nanoseconds (the duration of a single Q-switched laser pulse) to as long as 10 seconds (for a stream of laser pulses).

Many military laser systems operate at wavelengths within the near infrared. Of these, 1064 nm radiation is particularly hazardous to unprotected eyesight, due to the transparency of the atmosphere and the aqueous media at that wavelength. Laser energy of sufficient intensity at 1064 nm can cause permanent scarring of the retina, with significant loss of visual acuity. The NOHD for a typical airborne laser designator emitting at 1064 nm is on the order of tens of kilometers, a hazard distance that might be substantially increased once correction factors for magnifying optics and atmospheric propagation are taken into account. We should note that the general practice in UK NOHD calculations is to include a correction factor for atmospheric scintillation, but not attenuation. In contrast, US NOHD calculations generally include correction factors for atmospheric attenuation, but not scintillation.

An additional consideration in the hazard assessment is the angular spread over which laser energy may be fired. For airborne target designators and rangefinders especially, the wide field of regard of the laser steering mechanism, relative to the aircraft velocity vector, can produce a risk of laser energy being misdirected outside the CRA. A nominal hazard zone can be defined by sweeping the applicable NOHD over the angular range of possible directions in which the laser could be fired. It is necessary to implement adequate risk management procedures to

ensure that airborne military lasers with significantly large hazard zones can be operated safely within the context of an outdoor training or test Range. For a hazard assessment based on the MPE, such a requirement can be satisfied by ensuring either (a) that laser energy does not escape the CRA under any circumstances or (b) that the laser is never fired when an uncontrolled area outside the Range, where unprotected persons might be present, is within the appropriate NOHD.

Where sufficient real estate is available, it is possible to ensure confinement of the hazard zone within the CRA without imposing onerous restrictions on the permitted laser firing envelope. In such cases, the laser energy is said to have been “back-stopped” within the Range. US Ranges are typically large enough that back-stopping the beam is feasible, with the correct attack track and firing angle. Training Ranges within the UK, however, are generally small in extent – of the order of a few kilometers across – and the confined geography of the UK means that training Ranges are never very far from populated areas. Should hazardous levels of laser energy escape the confines of a Range in the UK for any reason, it is possible that an unprotected person could be exposed to laser irradiation in excess of the MPE. In such cases the zero risk criterion, implicit in standard risk analysis, creates a significant problem from the perspective of practical laser testing and training opportunities.

While the NOHD represents an appropriate safe exposure distance, the MPE-criterion provides no quantitative information on the probable risk of injury for unprotected observers inside the NOHD (i.e., in the hazard zone). Additionally, a strict implementation of the MPE safety standard across the entire laser field of regard does not take into account the possible variation in the risk of laser energy being fired in any given direction. With a well designed and properly calibrated laser directional control system, it would be expected that most – if not all – of the laser energy will be reliably incident on or close to the target. In most cases then, the risk of laser energy escaping the CRA will be small.

With the relatively small size of UK Ranges, the stringent limitations on the laser firing envelope, required to satisfy the MPE-criterion, could totally preclude practical testing of, or training with, airborne laser systems, even though the actual risk of injury may be negligible. This implies that standard MPE-based risk analysis is generally too inflexible for UK Range clearance requirements. Instead, UK Range clearance models are probabilistic, and based on the principle of residual risk being “As Low As Reasonably Practicable” (ALARP) [15]. The use of the ALARP principle in UK hazard assessment arises from the provisions of the UK *Health and Safety at Work Act* of 1974 [16]. Such requirements can only be satisfied by the use of a risk-based approach to laser hazard assessment. The outcome of such a risk-based assessment technique is a risk management process (see Fig.1), by which adverse events, and the inherent uncertainties with which they occur, can be rigorously identified and mitigated.

Figure 1 provides a schematic illustration of the UK risk assessment process, which comprises two distinct stages. The *risk analysis stage* constitutes a hazard assessment of the laser system *performance* when operating either as intended, or in the event of a laser sightline directional control system fault or failure. The laser system hazard assessment in the UK is expressed formally in a Laser Safety Paper (LSP), the production of which is the responsibility of the laser system project authority. The Probabilistic Range Clearance Model (PRCM) provides a means by which hazards arising from the laser system *operation* can be evaluated, and is necessarily based on the performance assessment described in the LSP. The PRCM represents the mathematical implementation of the “ $P_E$ - $P_I$ - $P_{OD}$ ” chain of adverse risk events model. An illustration of the “ $P_E$ - $P_I$ - $P_{OD}$ ” risk chain model, in a general risk modelling context, is provided in Figure 2 and further discussion of the risk chain model is provided in Section 2.2.

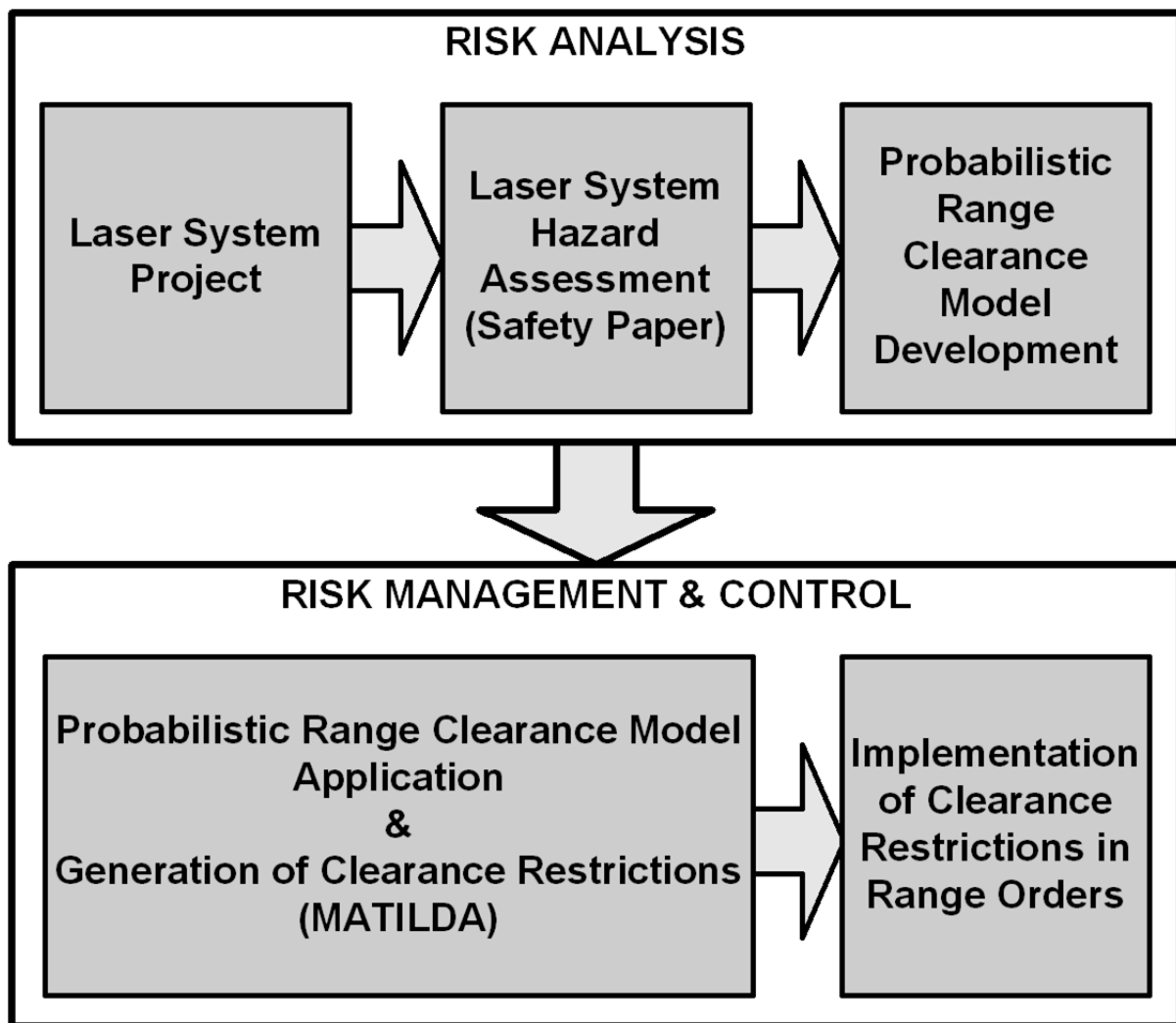


**Figure 1: Laser Safety Risk Management Process**

The hazard assessment for the laser system *operation* is the subject of the *risk management and control stage*. Laser firing restrictions for a given Range, target and attack profile combination are generated by application of the PRCM, as encoded in the MATILDA tool. The resulting restrictions on the permitted laser firing envelope may then be evaluated in context of other (non-laser) safety information, from which *actual* laser firing restrictions can be derived and promulgated to the system operators *via* Range orders. There are hence *two* separate hazard assessments encapsulated in Figure 1: the laser *system* hazard assessment as encapsulated in the LSP followed by the *operational* laser hazard assessment as effected by the PRCM application.

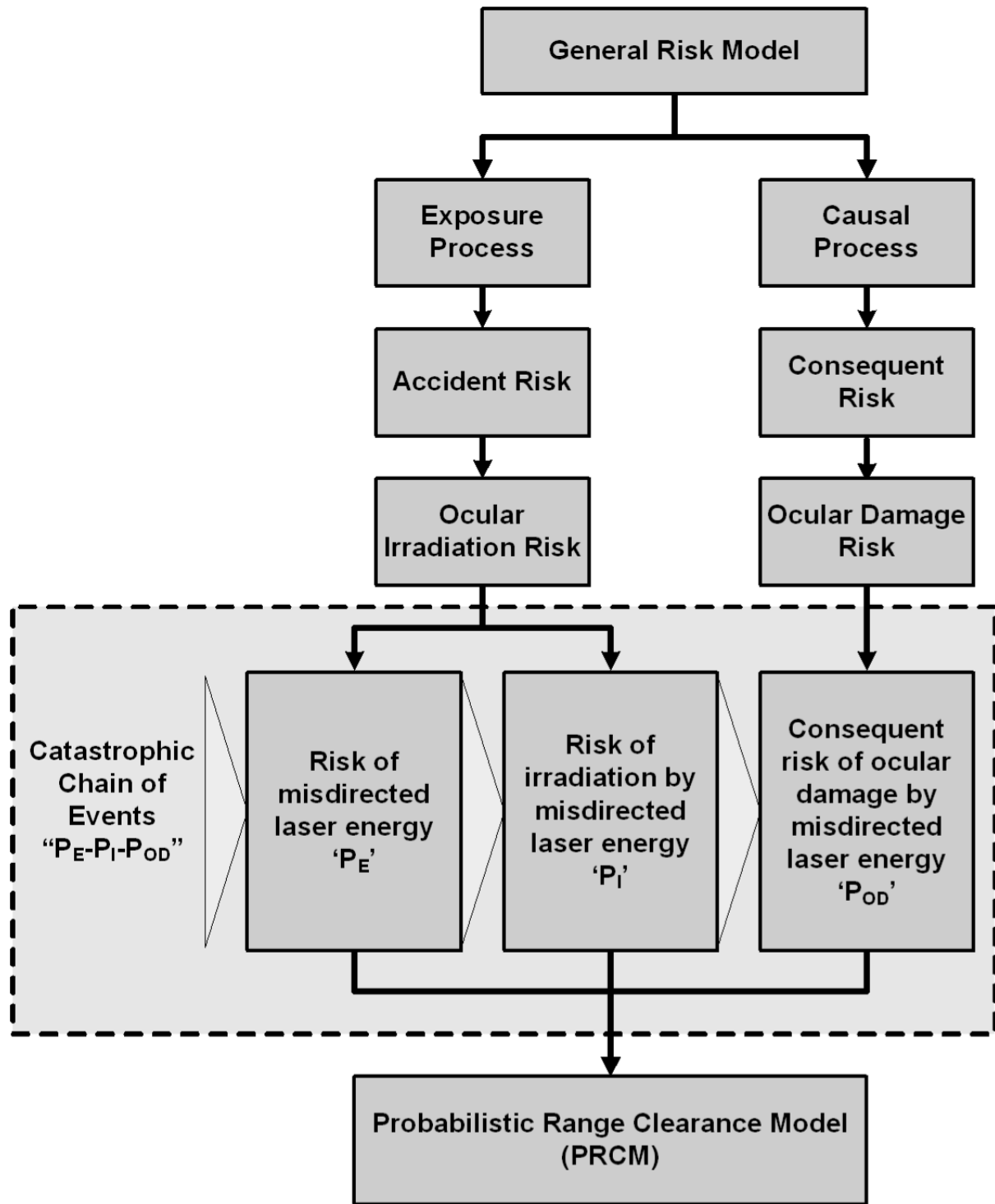


Figure 2: The “PE-PI-POD” Catastrophic Chain of Events Model

## 2.2 A Risk-Based Approach to Laser Hazard Assessment

The risk of an adverse event, such as a laser-induced ocular injury in an unprotected population, can be expressed in terms of a “risk chain” comprising three main components [17]: (i) a risk source, (ii) an exposure process and (iii) a causal process (see Fig. 2). In the case of airborne laser operations, the risk source is the laser. The exposure process is the means by which laser energy from an airborne platform could be misdirected outside the CRA, causing an unprotected observer to be irradiated. The causal process is the mechanism by which that misdirected laser energy could cause an ocular injury to the unprotected observer. Uncertainty persists within both the exposure and causal processes over the occurrence of given events, such as the misdirection of laser energy in a specific direction or the sustaining of an ocular injury.

Typically, the hazard posed by a risk event can be defined by the likeliness of its occurrence and its consequent impact [17]. The likeliness of an adverse event can be defined in terms of the frequency or probability with which it occurs. The impact of a given event depends on the extent to which the consequences of that event affect the system under consideration. In the case of an ocular injury, the impact can vary from minimal impact on visual acuity to a total loss of visual function. The bivariate relationship between likeliness and impact can be expressed in terms of a simple “quadrant” risk model, as illustrated in Fig. 3. In this simple model, an adverse event can occur with (a) a high likeliness but low impact, (b) high likeliness and high impact, (c) low likeliness and high impact, or (d) low likeliness and low impact.

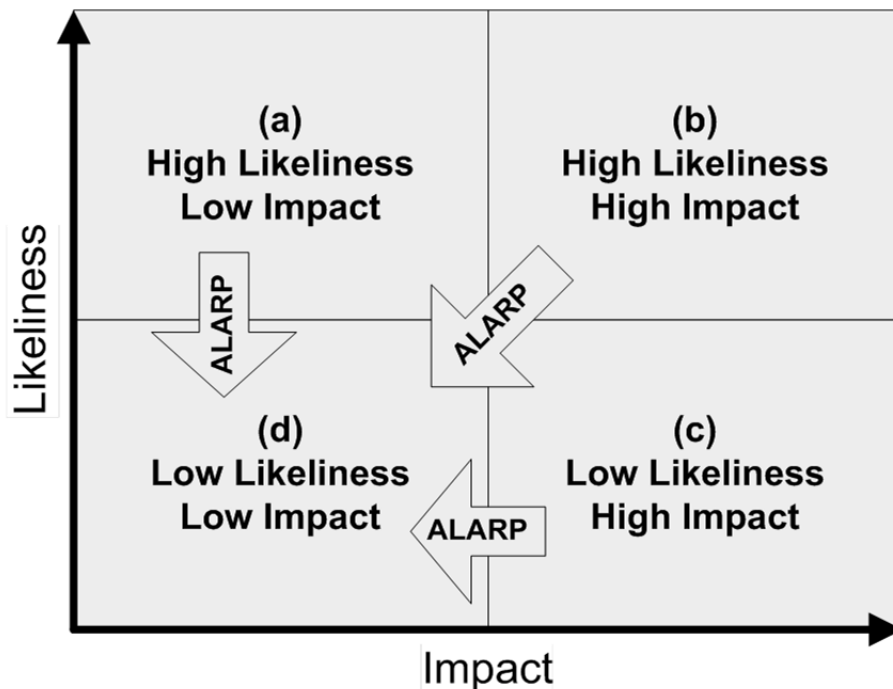


Figure 3: Risk Quadrant for an Adverse Event

The purpose of the ALARP principle is to identify and implement suitable risk management control procedures so as to ensure that any potentially adverse events occur only with a low likeliness and low impact. An important aspect of the risk-based approach is a suitable definition of what constitutes a low likeliness and low impact event. The likeliness of an event may be defined by a fixed value, for simple models, or by a Probability Distribution Function (PDF) for more complex ones. The General Risk Model thus falls naturally into a probabilistic structure, the “ $P_E$ - $P_I$ - $P_{OD}$ ” catastrophic chain of events structure, shown in Fig. 2. Here the “ $P_E$ - $P_I$ ” couplet represents the exposure process and the “ $P_{OD}$ ” element represents the causal process. The “ $P_E$ - $P_I$ - $P_{OD}$ ” structure provides the mathematical basis for the UK probabilistic laser hazard assessment.

As a start to constructing a mathematical model of the probabilistic laser hazard assessment, the risk chain must be broken down into its individual probabilistic elements. For airborne laser operations, the risk of ocular injury to unprotected persons can be characterised as the probability that a “catastrophic chain of events,” leading to an adverse outcome, will occur. The three main components of such a risk chain are: (i) the probability of laser energy being fired in an inappropriate direction outside the Controlled Range Area ( $P_E$ ), (ii) the probability of an unprotected observer being irradiated by the laser energy ( $P_I$ ), and (iii) the subsequent probability of the irradiated observer sustaining an ocular injury ( $P_{OD}$ ).

These three components can be further decomposed into five distinct elements: i) the risk of laser energy being directed outside the CRA; ii) the risk of an unprotected observer being irradiated; iii) the risk of the unprotected observer looking in the direction of the laser energy (ocular irradiation); iv) the risk of atmospheric scintillation increasing the radiant exposure entering the eye; and v) the risk of the received radiant exposure causing ocular damage. Here, the first element is associated with  $P_E$ , the second and third with  $P_I$ , and the fourth and fifth with  $P_{OD}$ .

Up to this time, UK risk-based Range clearance models have been based primarily on two of the three components: a probabilistic laser pointing error model ( $P_E$ ), coupled with a probabilistic ocular damage model for 1064 nm laser energy ( $P_{OD}$ ). These are described in more detail in Sections 2.3 and 2.4, respectively.

In contrast, due to the complexity of accurately determining the probability of an observer being at a particular location, or looking into the laser beam, the  $P_I$  component has usually been implemented in a highly simplified version. The probability of an observer being at a particular location, and the subsequent probability of that observer looking into the laser beam, is difficult to define, and is nominally set to unity for practical reasons. That is, it is generally pessimistically assumed that an observer is *always* irradiated when laser energy is directed outside the CRA and that that observer is *always* looking in the direction of the laser source. The inherent pessimism of this approach can then be mitigated by estimating the *expected number* of observers sustaining a given level of ocular damage in any given laser firing direction, based on the size of the beam footprint and the local population density.

## 2.3 Probabilistic Laser Pointing Error Modelling

The goal of probabilistic pointing error modelling is to identify a pointing error Probability Distribution Function (PDF), which quantifies the probability of laser energy being fired in any given direction. Clearly this function will vary, depending on the characteristics of the laser system and supporting aircraft being modelled. The UK probabilistic laser pointing error model addresses two separate regimes: (a) a “fault-free” regime, when the directional control system is operating as intended against a distinct well-defined target, and (b) a “fault/failure” regime, which covers situations when the directional control system fails to operate as intended. The latter might occur either as a result of an actual electro-mechanical failure, or due to a failure of the system to maintain the laser sightline alignment on the target, for example during rough weather, when the aircraft is an unstable platform.

Modelling of the fault/failure condition is an important feature of the UK’s risk-based Range clearance technique. A significant parameter is the probability,  $P_F$ , of a laser system fault or failure occurring during the course of a laser firing maneuver, which is expected to be low for a modern, well-maintained system. A suitable value for the probability of system fault or failure can be established using appropriate fault or failure data, including mean-time-between-failure (MTBF) statistics. It should be noted that the fault/failure condition covers only accidental or unintended laser pointing errors, and not deliberate firing of the laser outside of the Controlled Range Area. It is assumed and required that appropriate steps are taken to disable laser firing immediately after a fault or a failure has occurred, whether manually by the weapon systems operator (WSO) or automatically by built-in fault detection mechanisms. Consequently, it is expected that only a small amount of laser energy would potentially escape the confines of the CRA before laser firing ceases.

As mentioned, the definition of an appropriate PDF, covering the fault/failure condition, is dependent on the aircraft-laser system architecture. In particular, the maximum angular drift,  $\theta_{\max}$ , of a sightline error while the laser is still active will generally be a function of the system design and the WSO reaction time. In the absence of suitable statistical data, an appropriate distribution function for laser directional errors in fault/failure condition can be established through the use of simulation modelling. MTBF data is used, in conjunction with a simplified “onion-skin” model (see Fig. 4), to simulate the behaviour of the laser sightline following a fault or a failure in different parts of the airborne laser designator control system.

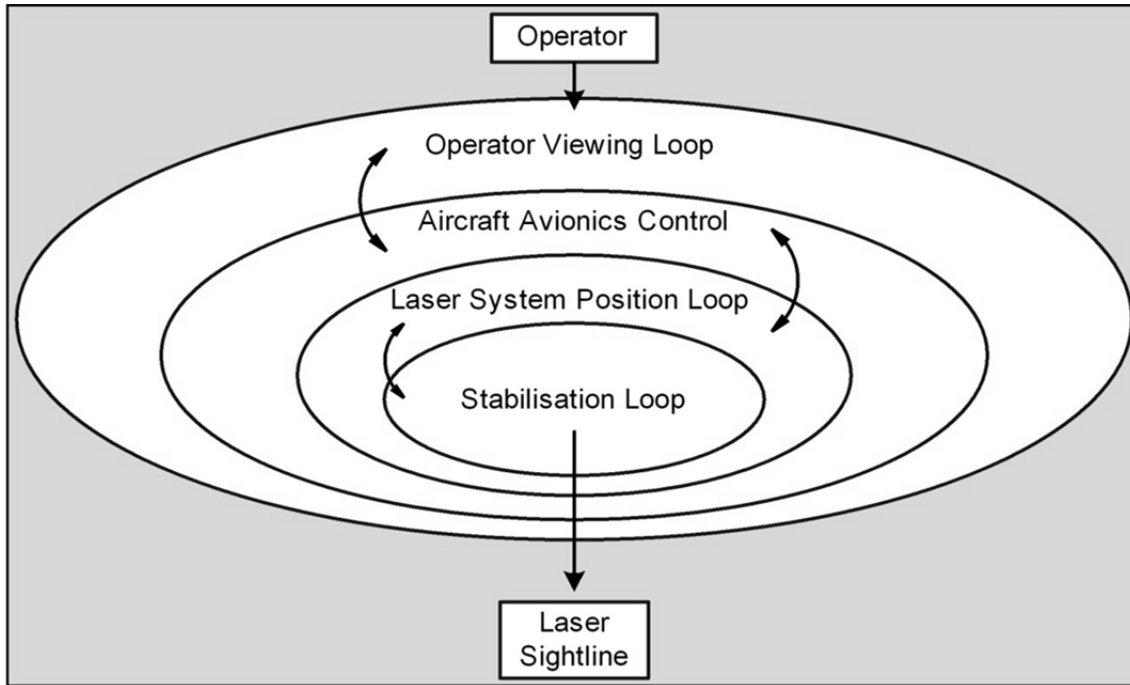


**Figure 4: The Selex ES “Onion-Skin” Fault/Failure Condition Model**

The distribution of laser pointing errors in a fault/failure condition depends on the laser system design and the consequences of any faults or failures that could occur in the directional control mechanism, all of which should be described in the LSP. Examples of directional control system failures include: a steering gimbals runaway, in which the laser sightline could be driven rapidly away from the target position, and a steering gimbals freeze, in which the laser sightline direction will depend on the aircraft motion relative to the target. Another possibility, depending again on the laser system design, could involve eccentric cycling of the laser sightline about the target as a result of a partial failure in the directional control system. The choice of statistical distribution representing errant laser sightline behaviour is hence dependent on the system design characteristics, together with the quality of information available for the analysis. Statistical functions that have historically been used to describe *simple* fault pointing error models (and which are or can be encoded in MATILDA) include the uniform, triangular and exponential distributions. More sophisticated analyses could alternatively be developed, depending on the resources available and the economic justification for doing so.

Fault-Free laser pointing errors are usually modelled as a circularly symmetric bivariate Normal distribution, which may be further expressed in terms of a radial pointing error,  $\phi$ . The associated PDF is given by considering the probability that a radial error lies in the annulus between the angles  $\phi$  and  $\delta\phi$  [18]. That is

$$\begin{aligned}
f(\phi) &= 2\pi \lim_{\delta\phi \rightarrow 0} \frac{P(\Phi < \phi + \delta\phi) - P(\Phi < \phi)}{\delta\phi} \\
&= \frac{2\phi}{\sigma_r^2} \exp\left\{-\frac{\phi^2}{\sigma_r^2}\right\}
\end{aligned} \tag{2.1}$$

which is the PDF for the Rayleigh distribution, where  $\sigma_r^2$  is the variance. The probability  $P(\Phi < \phi)$  is given by

$$\begin{aligned}
P(\Phi < \phi) &= \frac{2}{\sigma_r^2} \int_0^{\phi} t \exp\left\{-\frac{t^2}{\sigma_r^2}\right\} dt \\
&= 1 - \exp\left\{-\frac{\phi^2}{\sigma_r^2}\right\}
\end{aligned} \tag{2.2}$$

From the fault/failure probability,  $P_F$ , a maximum radial laser pointing error limit  $\alpha_{\max}$  may be evaluated, from which appropriate clearance restrictions on the ‘‘Fault-Free’’ laser firing envelope may be derived. That is

$$\begin{aligned}
P(\Phi < \alpha_{\max}) &= 1 - \exp\left\{-\frac{\alpha_{\max}^2}{\sigma_r^2}\right\} \\
&= 1 - P_F
\end{aligned} \tag{2.3}$$

$$\exp\left\{-\frac{\alpha_{\max}^2}{\sigma_r^2}\right\} = P_F \tag{2.4}$$

$$\alpha_{\max} = \sigma_r \sqrt{-\log_e P_F} . \tag{2.5}$$

In the UK model  $\alpha_{\max}$  is a maximum fault-free error, such that the probability of an excessively-large directional control error is small. It can be considered a threshold between normally-distributed fault-free laser pointing errors and fault/failure condition laser sightline errors.

## 2.4 Probabilistic Ocular Damage Modelling

The MATILDA tool currently uses the UK probabilistic ocular damage model, for 1064 nm laser energy, to assess the probability of injury for unprotected persons inadvertently exposed to stray laser radiation. The model is based on an experimentally-derived log-normal distribution relating total intra-ocular (laser) energy (TIE) with the probability of causing a Minimum Ophthalmoscopically Visible Lesion (MOVL) [3]. The UK probabilistic ocular damage model has also been combined mathematically with a probabilistic scintillation model, which predicts a

log-normal distribution for the multiplicative gain in laser energy density as a result of turbulence-induced atmospheric scintillation effects.

For the purposes of the UK probabilistic model, a MOVL is defined as a retinal lesion of 30  $\mu\text{m}$  diameter, assuming unaided viewing of the laser energy. The rationale behind this size of lesion is that: (a) it is practically the smallest lesion size that can be detected non-invasively using an ophthalmoscope, and (b) it is considered impractical for an infrared image smaller than 30  $\mu\text{m}$  to be formed on the retina, owing to the limitations of the human eye in imaging a distant infrared laser source. In the case of aided viewing of the laser source with magnifying optics, it is expected that the diameter of any laser image on the retina would be generally larger than the corresponding unaided image. Consequently, for aided viewing of the laser source, the MOVL diameter is increased to a value of 90  $\mu\text{m}$ .

An observer sustaining a MOVL on the most sensitive part of the retina (the fovea) could experience a minor but permanent impairment of visual acuity, such as a difficulty in reading fine print. A MOVL occurring on any other part of the retina, such as the macula or paramacula, may have even less effect on visual acuity. Given other (even naturally occurring) conditions that could seriously affect visual acuity, up to and including total blindness, the effect of a MOVL can be considered to be a low impact event.

It should be mentioned that probabilistic ocular damage models have also been developed independently by the US (AFRL). These are “dose-response” models which give the probability of causing a MOVL (response) as a function of exposure level (dose) for 1064 nm [19] and 1315 nm [20] laser radiation. The current plan is to include these US ocular damage models in more advanced versions of MATILDA, with the user given the option of choosing the appropriate model for their particular Range and training scenario.

## 2.5 UK Expectation Model

As described in Sections 2.3 and 2.4, the UK MOD has detailed probabilistic models for two of the three probabilistic components in the  $P_E$ - $P_I$ - $P_{OD}$  structure: i) a combined scintillation and ocular damage model for 1064 nm pulsed lasers ( $P_{OD}$ ) and a laser pointing error model ( $P_E$ ), which addresses both fault-free laser pointing errors and fault/failure condition laser sightline errors. By combining these with a suitable population distribution model, for a simplified  $P_I$  component, and with various laser system parameters, a stochastically-based “Expectation Model” may be constructed, which incorporates the  $P_E$ - $P_I$ - $P_{OD}$  structure.

The UK probabilistic hazard assessment model, or UK Expectation Model, is based on an evaluation of the expected number of unprotected observers who sustain a MOVL during an airborne laser firing maneuver, a quantity defined as  $E_{MOVL}$ . The Primary Criterion for clearance of a laser firing maneuver is that the expected number of cases of MOVL does not exceed a pre-defined maximum acceptable value,  $E_{MOVLMAX}$ . The Primary Criterion takes into account both the likeliness of laser energy being misdirected outside the CRA and the potential consequences of an unprotected observer being irradiated. Two additional precautions, the Secondary and Tertiary Precautions, are also implemented in the Expectation Model, to guard against the possibility of a low likeliness, high impact event, in which a high probability of ocular damage to

an irradiated observer could be masked by a low frequency of occurrence. This is known as “defense-in-depth.”

The overall expectation value,  $E_{\text{MOVL}}$ , of an unprotected observer sustaining a MOVL as a result of laser training operations on a Range, is evaluated in two steps: i) calculating the elemental (population-weighted) expectation value,  $e_{\text{MOVL}}$ , that an unprotected observer outside the CRA sustains a MOVL from a single pulse of laser energy, and ii) summing these single pulse expectation values over all pulses of laser energy fired during the operation to obtain the overall expectation value.

Now, if  $\Theta$  is a bivariate random variable representing the azimuth and elevation directions  $\underline{\theta}$  in which the laser could be fired relative to the laser–target vector and assuming  $n$  pulses of laser energy are fired during the attack, then for a real-valued function  $g$  [18],

$$E_{\text{MOVL}}(n) = \sum_{i=1}^n e_{\text{MOVL}}(g(r(\Theta))) \quad (2.6)$$

where  $g(r(\Theta))$  is a random variable representing the number of persons in the population suffering a MOVL as a result of laser training operations. In Equation 2.6, the single pulse expectation value  $e_{\text{MOVL}}$  is defined by

$$e_{\text{MOVL}}(g(r(\Theta))) = \iint_{\underline{\theta}} f(\underline{\theta}) g(r(\underline{\theta})) d\underline{\theta} \quad (2.7)$$

where  $f(\underline{\theta})$  is the laser pointing error PDF ( $P_E$ ) that gives the probability of a laser pulse being fired in the direction  $\underline{\theta}$ , and

$$g(r(\underline{\theta})) = n_p(r(\underline{\theta})) Q[w_{\text{MOVL}}(h(r(\underline{\theta})))] \quad (2.8)$$

represents the expected number of observers sustaining a MOVL as a result of this pulse. Note that the two factors in Eq. 2.8 represent the  $P_I$  and  $P_{OD}$  components of the risk model. The expected number of persons irradiated when the laser is fired in the direction  $\underline{\theta}$  is given by

$$n_p(r(\underline{\theta})) = \rho(\underline{\theta}) S(r(\underline{\theta})) \quad (2.9)$$

where  $\rho(\underline{\theta})$  and  $S(r(\underline{\theta}))$  are the local population density and the area of intersection of the laser beam with the ground plane, respectively. Once again we note that this is a simplified version of the  $P_I$  component, where the probability of an irradiation producing ocular exposure (probability of the observer looking into the beam) has been set to one.

The probability that an ocular exposure produces a MOVL ( $P_{OD}$ ) is given by

$$Q\left[w_{\text{MOVL}}(h(r(\underline{\theta})))\right] = \frac{1}{\sqrt{2\pi}} \int_{w_{\text{MOVL}}(h(r(\underline{\theta})))}^{\infty} e^{-\frac{t^2}{2}} dt \quad (2.10)$$

where

$$w_{\text{MOVL}}(h(r(\underline{\theta}))) = \frac{a\left(-\log_e(h(r(\underline{\theta}))) + \frac{\eta^2}{2}\right) + b(d)}{\sqrt{1 + a^2\eta^2}} \quad (2.11)$$

and

$h(r(\underline{\theta}))$  = the corneal laser energy density at distance  $r$  in the direction  $\underline{\theta}$  in  $\text{mJm}^{-2}$

$$a = 1.715$$

$$b(d) = 8.5169 + 3.73538 \log_{10} d$$

$d$  = the diameter of the laser image on the retina

$$= \begin{cases} 30\mu\text{m} & \text{for unaided (naked-eye) viewing} \\ 90\mu\text{m} & \text{for aided viewing with magnifying optics} \end{cases}$$

$\eta$  = standard deviation of log-irradiance

$$= 1.1$$

In a full probabilistic evaluation, the elemental expectations of ocular damage are evaluated for every pulse fired during the attack manoeuvre. An important feature of the full probabilistic method is the opportunity for ‘trade-off’ between the component probabilities. That is, it is possible for a high value in one parameter to be balanced by a low value in another. Hence, for example, a high probability that laser energy could irradiate a given area outside the CRA could be balanced by a low risk that anyone would be present within that area.

Once the overall expectation value,  $E_{\text{MOVL}}$ , has been evaluated, it must be compared with the Primary Criterion,  $E_{\text{MOVLMAX}}$ , which defines the maximum acceptable risk of ocular damage occurring in the population during laser training operations. If the Primary Criterion is exceeded, then restrictions on the laser firing envelope are imposed to reduce risk to acceptable levels. A typical maximum acceptable expectation value for UK Range clearances is  $10^{-8}$  occurrences of MOVL per attack. In comparison, a typical NASA acceptable expectation value, for injury by falling inert debris, is  $10^{-6}$  injuries per launch. Note that the very low risk levels set by the Primary Criterion are principally achieved by ensuring that most of the laser energy falls within the CRA. Once the Primary Criterion is met, then the Secondary and Tertiary Precautions are applied, to identify any additional restrictions on the laser firing envelope.

The Secondary Precaution evaluates the expected hazard for a scenario in which it is assumed that laser energy is misdirected towards a populated area outside the CRA. The acceptable criterion for the Secondary Precaution is that – should laser energy be inadvertently misdirected outside the CRA – the expected number of cases of MOVL does not exceed a maximum *conditional* expectation value,  $E_{\text{CONMAX}}$ . For the UK, a typical maximum value for the Secondary Precaution is on the order of  $10^{-3}$  to  $10^{-4}$  occurrences of MOVL per attack. Finally, the Tertiary Precaution assumes that an unprotected observer has actually been irradiated by a

single pulse of laser energy. The acceptable criterion for the Tertiary Precaution is that the probability of a MOVL for an irradiated individual does not exceed a pre-defined maximum value,  $P_{\text{MOVLMAX}}$ . For the UK, a typical maximum value for the Tertiary Precaution is  $10^{-1}$  occurrences of MOVL per attack.

Appropriate restrictions are imposed on the laser firing envelope to ensure that the Primary Criterion, Secondary Precaution, and Tertiary Precaution, are all satisfied. The effect of the Tertiary Precaution is to impose a probabilistically defined Minimum Separation Distance (MSD) between the laser and any unprotected observer outside the CRA. The MSD is applied in *all* directions in which the laser *could be* fired before the laser operation is inhibited either automatically by the laser system itself, or manually by the operator. In this respect, the MSD is similar to the NOHD, albeit much smaller in magnitude. An unprotected observer located at the MSD from the laser would be at a non-zero risk of sustaining a given measureable level of ocular damage, if irradiated. The role of the MSD is similar to that of a seat-belt in a car. The purpose of a vehicle seat-belt is to provide the occupant with a degree of protection against the possibility of a more serious injury in the event of an accident: its primary role is to mitigate the possible consequences of an accident *to an individual* rather than provide total protection against injury or death. In a similar manner, the purpose of the MSD is to ensure against the possibility of more serious levels of ocular damage should an *individual observer* be irradiated.

## 2.6 UK Partition Model

The UK Partition Model is a specific implementation of the UK Expectation Model described above, in which the hazard contributions arising from fault-free and fault/failure operation of the laser directional control system are “partitioned” and evaluated separately. The overall clearance restrictions defining the permitted laser firing envelope are a composite of the separately and sequentially evaluated restrictions for fault-free and fault/failure operation. As mentioned previously, the Partition Model described here, and used in the MATILDA tool, was developed to perform Range safety clearances for the UK TIALD system.

The Partition Model is fundamentally a geometric implementation of the hazard analysis, based on where in the terrain laser pulses are expected to fall. Laser pulses emitted during fault-free laser operation, which will be the majority of pulses fired during most attack runs, will be constrained to fall within the CRA by geometric restrictions on aircraft operations generated during the fault-free analysis. Consequently, any hazard to the population surrounding the Range will come from the relatively small number of pulses which could be emitted during fault/failure operation and which might fall outside the CRA. The hazard from these pulses is determined using the full probabilistic Expectation Model described in Section 2.5

A Fault-Free Laser Firing Zone (FFLFZ) is a geometric area within which an aircraft flying at a designated altitude can fire freely at the target. For any given attack altitude, the FFLFZ is defined in such a way that all fault-free laser pointing errors (errors less than  $\alpha_{\text{max}}$ ) produce laser beams that fall within the CRA. Typically, the FFLFZ are evaluated for all compass directions around the target, and over a range of aircraft altitudes, in accordance with laser system user requirements. Each designated aircraft altitude produces a different FFLFZ. The geometry of the

FFLFZ calculation is similar to the standard risk analysis methods currently used by the USAF to establish a safe laser firing envelope [11]. However, the FFLFZ calculation is designed to maximise the range-to-target at which the laser can be fired, given the extent of Controlled Range Area available.

The hazard analysis for fault/failure operation is the fully probabilistic portion of the overall laser hazard assessment. It follows computation of the FFLFZ, considers laser pointing errors in excess of  $\alpha_{\max}$ , and is only performed for specific laser firing maneuvers on specific aircraft attack tracks. Thus, the first step in the fault hazard analysis is to define the aircraft attack track, attack altitude, and laser firing positions. A check is then made to ensure that the attack scenario complies with FFLFZ restrictions. Any laser firing maneuvers which do not comply with FFLFZ restrictions are eliminated prior to the fault hazard analysis. Next, the probabilistic Expectation Model is used to evaluate  $E_{\text{MOVL}}$ , and this is compared to the maximum acceptable value,  $E_{\text{MOVLMAX}}$ , to determine whether the specified laser firing maneuver meets the Primary Criterion for safety clearance. Finally, if the Primary Criterion is met, then the Secondary and Tertiary Precautions are applied, to identify any additional restrictions on the laser firing envelope.

The Partition Model is a means by which the conditional expectation of a MOVL in an unprotected population can be evaluated, and appropriate laser firing restrictions defined, such that risks produced by a specified laser firing maneuver are kept within acceptable limits. In terms of the quadrant risk model (Fig. 3), the FFLFZ ensures that all high likeliness events, whether of high or low impact, are contained within the controlled Range area. Furthermore, the subsequent fault hazard analysis ensures that appropriate additional restrictions are defined to avoid the occurrence of low likeliness, but potentially high impact events. In this respect, the Partition/Expectation Model satisfies the ALARP requirement.

## 2.7 Computational Model

The Partition/Expectation Model is implemented by means of the Computational Model, from which the applicable laser firing restrictions are derived. The Computational Model is composed of three main modules, executed sequentially, called RBPROG, CALCZONE, and CALCFAULT. In these modules input data required for the hazard assessment – such as Range boundaries, terrain elevation data, target position on the Range, local demographics, local geography near the Range, and aircraft and laser system parameters – are first specified. Appropriate preliminary computations, including definition of the Controlled Range Area (CRA), are then performed, followed by the execution of the Partition model as described above.

The initial module is the Range Boundary Program, known as RBPROG for short. The main purpose of the RBPROG algorithm is to define the Controlled Range Area, which will be used in the CALCZONE module to define the FFLFZ. The CRA is a sub-set of the total Range area, which is “star-shaped” with respect to a given target. A CRA is defined to be star-shaped when any radial,  $\omega$ , emanating from the target, crosses the Range boundary only once. Frequently the initial Range area does not satisfy the star-shaped condition, so a portion of it is truncated to

form the star-shaped CRA. Extra coordinates are also inserted around the modified CRA boundary to provide appropriate computation points for the CALCZONE algorithm.

The second module, CALCZONE, performs the fault-free laser hazard analysis. Specifically, it calculates the FFLFZ for each designated target within the CRA, and for each designated aircraft altitude. The definition of an FFLFZ begins with a set of radials connecting the target to each of the CRA boundary points. For each radial,  $\omega$ , emanating from the target, CALCZONE computes a maximum laser firing range-to-target (ground range),  $R(\omega)$ , such that fault-free laser pointing errors (within  $\alpha_{\max}$  of the laser-target vector) remain within the CRA. This requirement results in two such ranges-to-target,  $R_u(\omega)$  and  $R_o(\omega)$ , corresponding to the need to keep “undershoot” and “overshoot” laser pointing errors, respectively, within the CRA, as shown in Fig. 5. We should note that azimuth errors are generally not significant compared with elevation (i.e. undershoot or overshoot) errors. We should also note that Fig. 5 shows the aircraft firing when not directly over the Range, something not usually done during US laser Range tests. This is allowed under UK laser safety policy, due to their small Ranges, but only on fixed approaches and at fixed heights, as indicated by the Fault-Free Laser Firing Zones (FFLFZ).

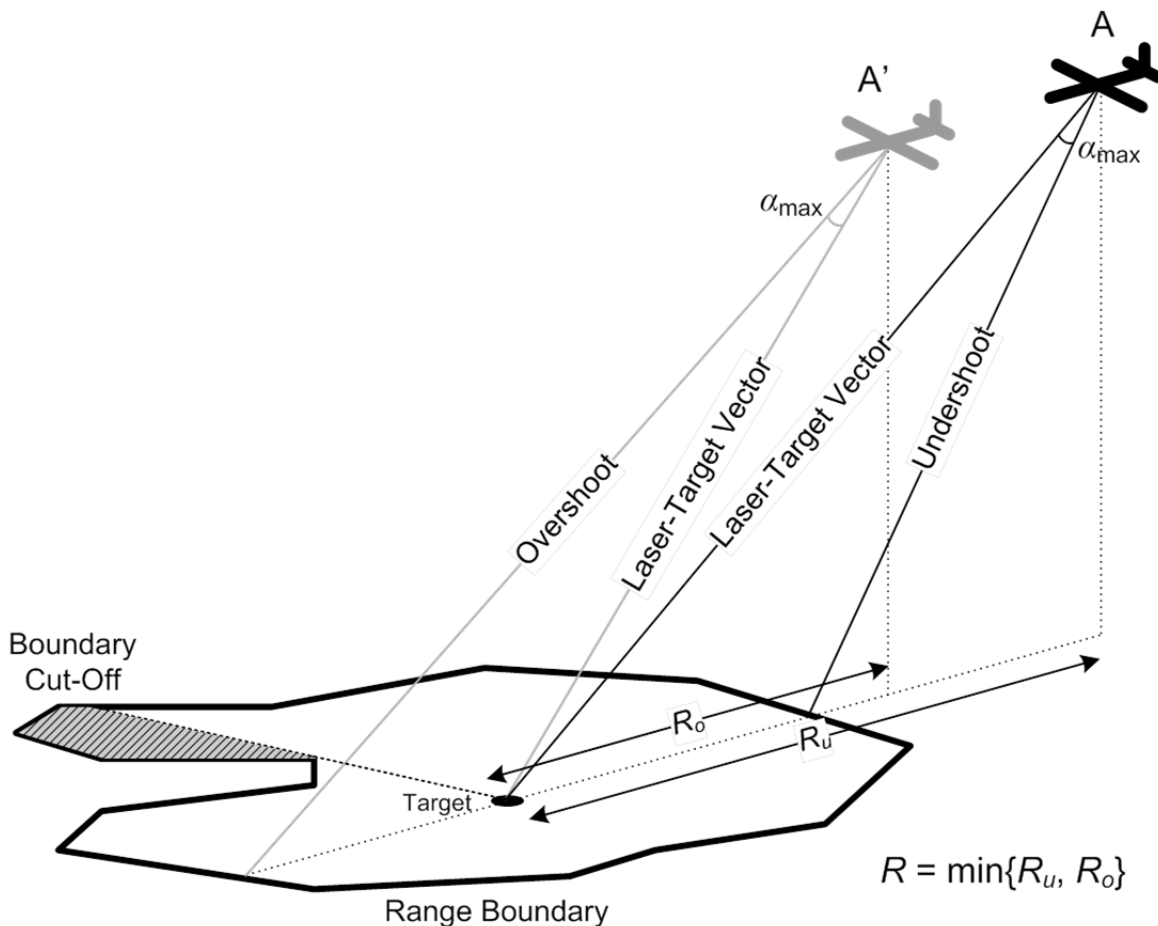


**Figure 5: Fault-Free Overshoot & Undershoot**

The applicable maximum range-to-target,  $R(\omega)$ , at which the laser may be fired is taken to be the smaller of the undershoot and overshoot ranges; that is,  $R(\omega) = \min\{R_u(\omega), R_o(\omega)\}$ . Since the firing angle to the target will vary with aircraft height (or altitude),  $H$ , a different set of maximum firing ranges will be obtained for each designated aircraft altitude. The FFLFZ for each aircraft altitude can then be defined as the set  $\{R(\omega): \omega \in [0, 2\pi)\}$ . For any aircraft maneuver, at any given altitude, the FFLFZ defines the maximum range-to-target at which the laser may be fired, assuming fault-free operation of the laser directional control system.

The third module, CALCFAULT, performs the probabilistic fault/failure hazard analysis for a specific laser attack scenario, to determine if any additional restrictions must be imposed on the laser firing envelope permitted by the FFLFZ. As mentioned previously, the first step in the fault hazard analysis is to define the aircraft attack track, altitude, and laser firing positions. A check is then made to ensure that the laser attack scenario complies with FFLFZ restrictions and any laser firing maneuvers which do not comply are eliminated.

Since a fault/failure could occur at any point during the course of the cleared laser attack scenario, a large number of failure cases, each representing a possible failure of the directional control system at a different point along the attack track, must potentially be evaluated and their overall expectation values compared to the Primary Criterion. Generally, the number of failure cases evaluated is equal to the number of pulses fired during the attack scenario; i.e., the fault hazard analysis is performed for a possible failure at each of the laser firing positions. For each laser pulse emitted after the fault/failure, the CALCFAULT algorithm evaluates a corresponding expectation value,  $e_{\text{MOVL}}$ , that a MOVL will occur in the unprotected population surrounding the CRA. The number of pulses emitted after a fault or failure has occurred depends on the pulse repetition frequency (PRF) and the length of time required for the laser to cease firing. Consequently, the overall expectation value,  $E_{\text{MOVL}}$ , for a particular failure case, is the sum of the individual pulse  $e_{\text{MOVL}}$  values for the period of time during which the laser continues to fire, and before laser firing is inhibited.

Restrictions on laser firing are subsequently imposed on those portions of the aircraft attack track for which the calculated value of  $E_{\text{MOVL}}$  exceeds the acceptable limit. Additional laser firing restrictions may also be imposed on those portions of the aircraft maneuver that bring the laser to within the applicable MSD of potentially vulnerable populated areas. The Computational Model requires a significant amount of geographic and demographic data in order to compute an optimum set of restrictions for any given laser firing operation during a training maneuver. The MATILDA tool is designed to provide a suitable software platform for performing these calculations and displaying the results, based on geographic information system technology tailored to the needs of airborne military laser hazard assessment.

### **3 THE MATILDA TOOL**

#### **3.1 Genesis of MATILDA**

During the early 1990s, the USAF identified the need for an automated software tool to aid Range Safety Officers in establishing laser Range safety clearances. The result was the Laser

Range Management Software (LRMS) tool, which the USAF's Optical Radiation Safety team has used for nearly two decades to establish MPE-based Range safety clearances for all of the USAF active Ranges. During the late 1990s, the USAF began attempts to understand the safety implications of developing High Energy Laser systems. Initial developments followed the accepted standard risk analysis approach, but it was recognized by AFRL that eventually a PRA-based tool would be necessary to deal with HEL hazard analysis in support of Range testing, training, and operational deployment. It was at this time that discussions with the UK MoD began, with the goal of leveraging their laser PRA modelling capabilities.

Early discussions focused on each organization's respective methodologies for laser safety and hazard analysis. After consideration, it was agreed that the best way to clarify US understanding of the UK PRA-based approach was to actually implement one of the existing UK models, using AFRL expertise in development of advanced software tools for laser hazard analysis. By approaching the collaboration in this manner, the USAF has realized its goal of understanding UK methodology, and the UK has realized its goal of obtaining an integrated version of their laser PRA analysis methodology in a single analytical tool. It was decided that the best candidate for this effort would be the PRA partition model for the UK Thermal Imaging Airborne Laser Designator (TIALD) system. The UK also suggested that the new software be called the Military Advanced Technology Integrated Laser hazard Assessment (MATILDA) tool.

### **3.2 MATILDA Development and Testing**

The UK MoD's TIALD model consisted of several HP BASIC programs that had been developed and refined over many years. Each program was a stand-alone code whose results were manually fed to the next program in the analysis chain. Geographic input data were manually extracted from British Ordnance Survey maps. Although an independent implementation of TIALD model algorithms has been created in MATILDA, the results of these original codes have proven valuable as a cross-check on MATILDA results.

During MATILDA development, the UK MoD has supplied the mathematical models, algorithms, and corresponding documentation, while the USAF has been the primary software developer. A lesson learned from earlier generations of laser codes was to encapsulate computational logic/code into a non-proprietary language to avoid continuous porting of the code to the latest fad in software tools. FORTRAN has long been that language but has been losing ground to C and C++ over the last couple of decades. Thus MATILDALib is an ANSI C++ library that encapsulates all of the computational code and logic required of RBPROG, CALCZONE, and CALCFAULT. Using C/C++ provides MATILDALib the speed advantages inherent in C/C++ codes while also providing portability to most modern computing platforms.

Although MATILDA started out as a computational tool, and retains a computational focus, the need to display the results graphically became readily apparent during the initial implementation of the RBPROG algorithms. The original HP BASIC codes implemented a scaled version of the British National Grid Coordinate system. Early discussions between the UK MoD and USAF had already emphasized the need to leverage standard Geographic Information System (GIS)

format; however, budgets on both sides were limited. Fortunately for us, the Idaho State University (ISU) Geospatial Software Lab (GSL) had similar constraints several years earlier, when they launched the MapWindow Open Source development effort. After a quick study of the ISU GSL capabilities, it was decided that MATILDA should consist of a set of plug-ins to MapWindow.

The MATILDA development team has made a concerted effort to keep the computational engine of the tool, MATILDALib ANSI C++, completely independent of the MapWindow code. Separating the Graphics User Interface (GUI) from the computational engine has a number of advantages. It simplifies coding, de-bugging, and updates of the different modules of the tool, enhances portability to different platforms, and allows MATILDALib to be leveraged by any GIS application/system. This is important because, just as the MATILDA project has leveraged MapWindow efforts, future PRA applications will be able to leverage the MATILDA effort.

Due to the differing requirements for generating Range clearance information, it was agreed that there should actually be three different versions of MATILDA. The first (MATILDA “User”) would be for basic users, to simply determine whether a particular mission was allowed, based on an established Range clearance, and with little or no ability to change any of the previously verified and tested input parameters. The second (MATILDA “User Plus”) would be for a more advanced user at the Range, to incorporate limited changes to the target position and attack track. The third (MATILDA “Pro”) would be the full model for expert analysts, who would be responsible for setting the parameters needed for the Range safety analysis and then performing the analysis to establish the initial Range clearance.

A detailed description of the algorithms and analysis procedures used in each of the three main MATILDA computational modules, RBPROG, CALCZONE, and CALCFAULT, is given in Sections 3.4 to 3.6, respectively. In addition, to illustrate the results given by each module, MATILDA Pro Version-1.6.2 was used to perform a hazard analysis for a sample case: a hypothetical airborne laser designator used in an attack maneuver during a training scenario at the UK’s Tain Range in northern Scotland. Prior to execution of the three main modules, however, a large amount of data must be input, and some data transformations and set-up procedures must be completed. Thus, in Section 3.3, we begin our detailed description of code operations by describing the types of input data, data transformations, and set-up procedures required to initiate a MATILDA analysis, as well as the sample case used for illustration.

### **3.3 MATILDA Inputs, Set-Up Procedures, and Sample Case**

There are five types of input data required for a full MATILDA analysis: i) population data for the urban and rural areas surrounding the Range; ii) laser system parameters; iii) aircraft attack track data; iv) terrain mapping and terrain elevation data; and v) geometric and geographic data defining the range and areas surrounding it. The latter includes Range boundaries, target position on the Range, location and boundaries of Urban Areas, and natural geographic features such as rivers, lakes, and coastlines. Both the Urban Areas and the initially defined Controlled Range Area (CRA) must be represented in the input data by predefined closed boundary polygons. The closed boundary polygon defining the initial CRA may represent the boundary of the total Range

area, or may be some subset of it, constructed by the analyst using other natural and man-made geographic features such as roads, fences, and coastlines.

The five data types described above may initially be available to the analyst in a variety of physical units. For consistency a single system of units must be used in computations. The Meters, Kilograms, Seconds (MKS) unit system has been chosen for MATILDA and, with some specific exceptions, all data not initially available in MKS units are transformed into them prior to input. Another potential problem is that the latter three data types (items (iii) – (v) above), being geographic in nature, may initially be available in a variety of coordinate systems, typically local (grid-based) map coordinate systems. For computational consistency these are transformed into a single common coordinate system, termed the MATILDA Internal Coordinate System (MICS). In order to bring such local map data into the MICS, three different coordinate transformations are performed, as shown schematically in Fig. 6.

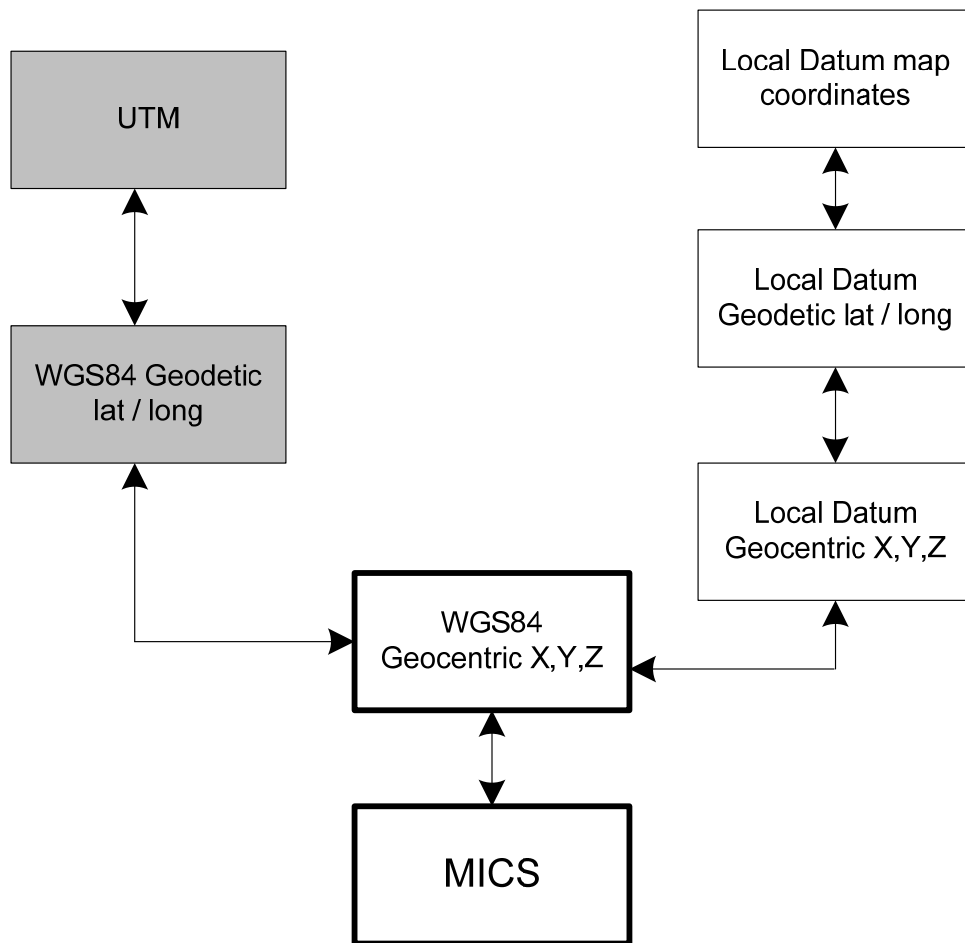


**Figure 6: MATILDA Coordinate Transformations**

The full mathematical details of the coordinate transformations listed in Fig. 6 are beyond the scope of this report; but may be found in Annex A of Ref. [18]. Here we give only a brief

summary of the transformation process. The local map coordinates are transformed first into Geodetic (latitude, longitude, altitude) coordinates. Next the Geodetic coordinates are transformed into Geocentric coordinates, a Cartesian (x,y,z) coordinate system with origin at the center of the Earth and z-axis oriented towards the North Pole. Finally Geocentric coordinates are transformed into the MICS, which is a Cartesian coordinate system local to the Range, where x is east, y is north, z is up, and the origin is at the target center. Fig. 7 illustrates the relationship between Geocentric and MICS coordinates.

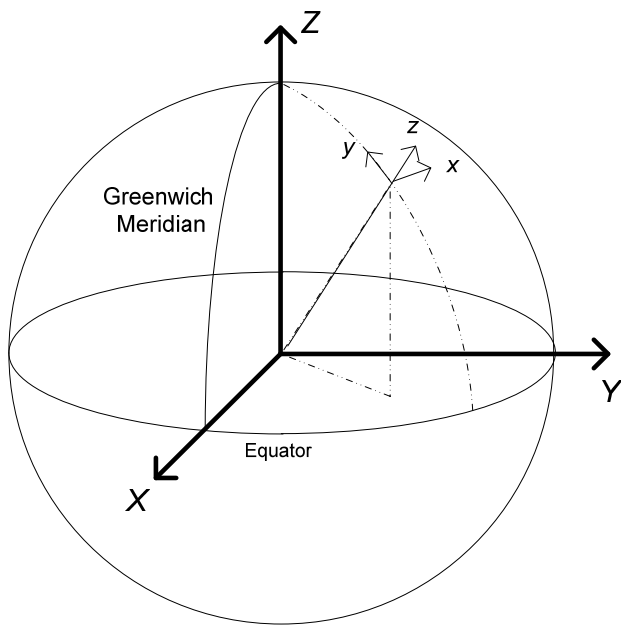


**Figure 7: Geocentric and MICS Coordinates**

Referring once again to Fig. 6, we should note that WGS84 is the Global Positioning System (GPS) standard which is used by most current global mapping systems. The transformations bring data from all sources to a common WGS84 Geocentric system and then transform this data into MICS. When computations are completed, Range clearance data must be transformed from MICS back into a local map coordinate system, using the right-hand path of the Figure. Working backwards, MICS is transformed into WGS84 Geocentric, then into WGS84 Geodetic, and finally into local map coordinates using the Universal Transverse Mercator (UTM) map projection. The latter has been used by the U.S. military to map a considerable portion of the Earth's surface.

After data input and data transformations are complete, there is one additional set-up procedure which must be performed prior to initiating the MATILDA analysis with RBPROG: generation of a mathematical model termed the Terrain Profile Surface, using the digital terrain elevation data and target location supplied. The Terrain Profile Surface is a simplified representation of the terrain elevation in the area surrounding the target. This theoretical surface has the target location as its lowest point. From that point it rises, in terrain steps of steadily increasing height, as we move radially outward from the target in all directions. Terrain step heights are defined

within an angular sector at given radial distances from the target. Figure 8 illustrates a sample terrain profile “web” in which the terrain steps are defined at one kilometer radial intervals, within 10° sectors centered on the target. The CRA boundary is indicated by a dashed line. The height of each step in an angular sector is defined by the maximum spot height of the terrain lying beneath that step, or by the height of the previous step nearer the target, whichever is greater. The end result is that the surrounding terrain heights are always below the surface.

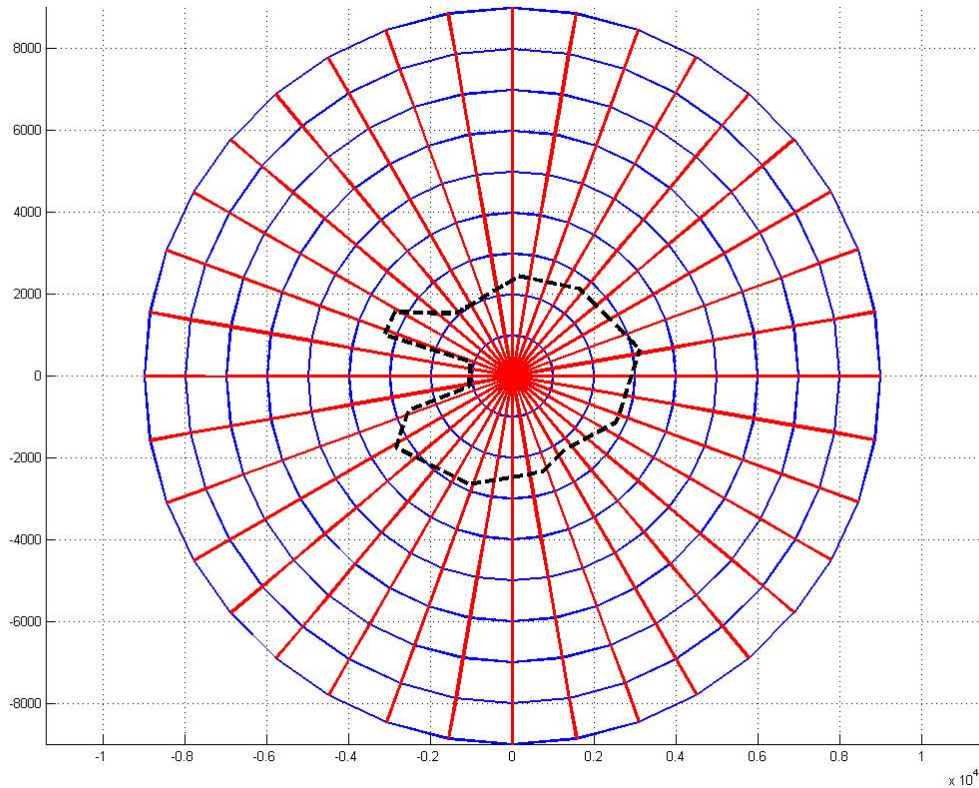


**Figure 8: Terrain Profile “Web”**

The Terrain Profile Surface provides a means of ensuring against the possibility of short-range irradiation of elevated terrain areas under the laser—target vector, where unprotected persons might be present. It is used in the CALCZONE module, to aid in the proper definition of the Fault-Free Laser Firing Zones (FFLFZ), which can be affected by the underlying terrain step profile. This will be discussed in more detail in Section 3.5.

We conclude Section 3.3 by describing the sample case which will be used to illustrate the results of the main MATILDA modules in the next three sections: a hypothetical airborne laser designator used in an attack maneuver during a training scenario at the UK’s Tain Range in northern Scotland. For this sample case it is assumed that the hypothetical airborne laser

designator is a multiple pulse “all-round line-of-sight” system mounted on a single-seat strike aircraft.

Important laser input parameters include: i) pulse energy, peak irradiance, and beam energy distribution; ii) other key beam parameters such as wavelength, beam divergence, pulse duration, and pulse repetition frequency; iii) Fault-Free and Fault Pointing Error Distributions; and iv) the Probability of Fault for the laser system. These laser system parameters are obtained by the laser system manufacturer, through testing of multiple laser units and averaging of performance data. The data is provided to laser safety officers in the Laser Safety Paper (LSP), described in Section 2.1. The laser system input parameters for our sample case are summarised in Table 1.

**Table 1: Input Parameters for the Hypothetical Airborne Laser Designator**

<b>Parameter</b>	<b>Parameter Value</b>
Fault-Free Pointing Error Distribution	Gaussian
Fault-Free RMS Pointing Error	5 mrad
Fault Pointing Error Distribution	Uniform
Maximum Fault Pointing Error	0.35 rad (20 deg)
Probability of Fault	$10^{-4}$ per attack
Laser Switch-off Time in Fault Condition	3 seconds
Laser Wavelength	1064 nm
Pulse Energy	200 mJ
Beam Divergence	0.124 mrad
Pulse Duration	10 ns
Pulse Repetition Frequency	20 Hz

In addition to laser system parameters, geographic input data were also loaded for our sample case, including Range boundaries for the Tain Range (equivalent to the initial CRA), target position on the Range, location and boundaries of nearby Urban Areas, and local terrain and coastlines near Tain Range, which borders on the North Sea. Geometric inputs of this kind are represented visually by shapes on layers loaded by the analyst, and the results for this case are shown in Fig. 9. Terrain elevation data for the region surrounding Tain Range were also input and used with the target location to create the Terrain Profile Surface, and population data were input for each of the nearby Urban areas. Data on the aircraft attack track were not input until the end of the CALCZONE module, as discussed in Section 3.5. Once data input and set-up procedures are complete, the three main modules, RBPROG, CALCZONE, and CALCFAULT, are executed sequentially.

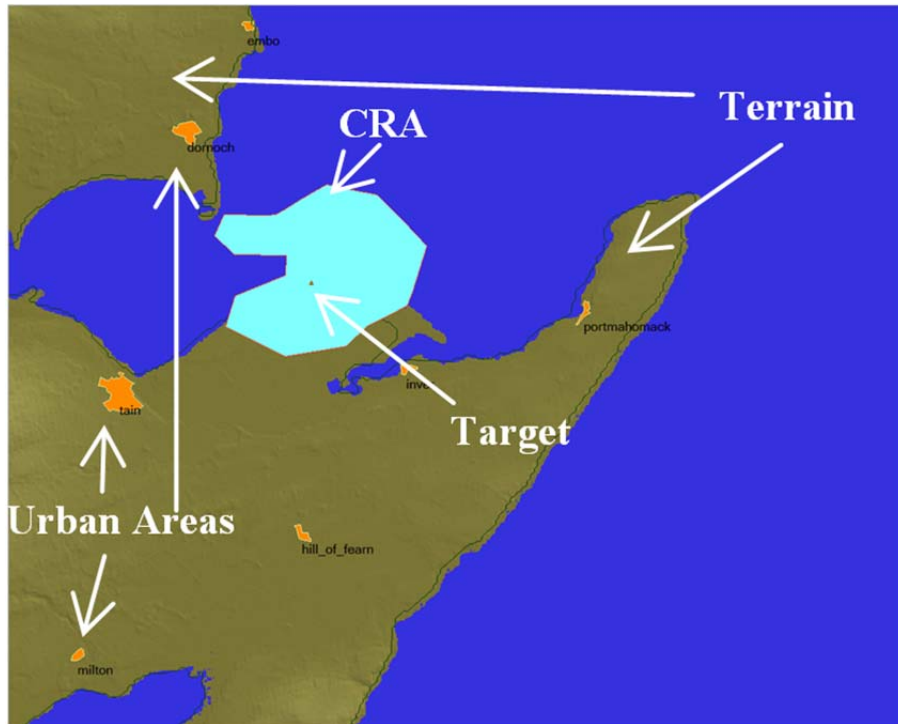


**Figure 9: The MATILDA Pro Primary Geographic Inputs**

### 3.4 RBPROG Analysis

The main purpose of the RBPROG module is to define a Controlled Range Area (CRA) which is suitable for use in the CALCZONE module, where the Fault-Free Laser Firing Zones (FFLFZ) are defined. The initially defined CRA, input during code start-up, may or may not be suitable for CALCZONE. A suitable CRA is defined to be a sub-set of the initial CRA which is “star-shaped” with respect to a given target; i.e., any radial emanating from the target crosses the CRA boundary only once. The RBPROG analysis achieves a suitable CRA with 6 steps: i) the “star-shaped” condition, ii) the “points of closest approach” condition, iii) the “terrain profile” condition, iv) the “urban area” condition, v) the “small increment” condition, and vi) the “undershoot/overshoot” condition.

As stated above, the star-shaped condition ensures that any radial drawn outward from the target position crosses the CRA boundary only once. To assess the star-shaped condition, we first assume that the boundary points for the initial CRA are listed in a counter clockwise direction relative to the target; i.e., with angular bearings increasing from 0 to 360 degrees. If the bearings of each consecutive boundary point form a strictly increasing set, then the CRA is star-shaped. On the other hand, if at any point the bearing decreases, before increasing again, then a ‘switch-back’ has occurred and the CRA is not star-shaped. The presence of a switch-back indicates that a radial line from the target can cut the CRA boundary at more than one point. The star-shaped algorithm identifies and removes switch-backs from the list of CRA boundary points. In removing a switch-back, a new boundary co-ordinate is created and inserted into the appropriate

point in the list. All subsequent boundary co-ordinates, up to the point where the switch-back ends, are removed from the list. Figure 10 illustrates this concept for Tain Range and shows that part of the initial CRA area is excluded to satisfy the star-shaped condition.

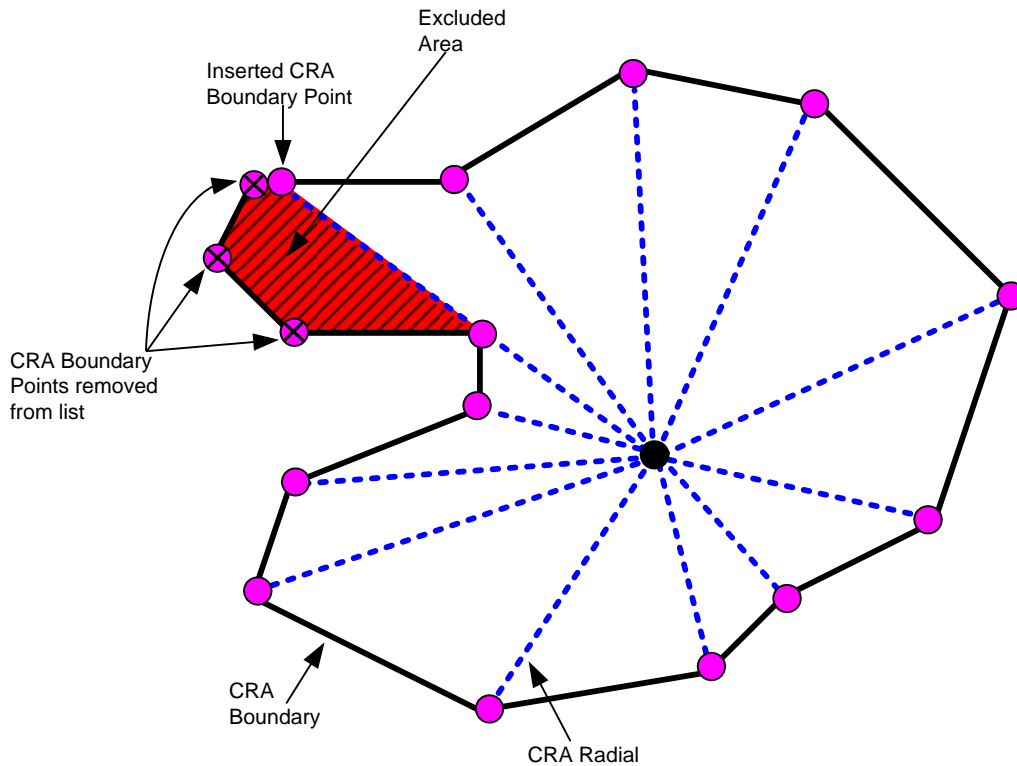


**Figure 10: Star-Shaped Condition**

For any CRA boundary line segment, the point of closest approach between the Range boundary and the target sets the worst case minimum safe firing range for the aircraft. The purpose of the points of closest approach condition is to insert CRA boundary points at the point of closest approach for each line segment, unless these points are already in the CRA boundary list. These additional boundary points are used in CALCZONE to ensure that a Fault-Free Laser Firing Zone contour point is calculated for each worst case minimum safe firing range. The point of closest approach for a line segment will be either: i) one of the two end points of the line segment, or ii) the point of intersection between the line segment and the target normal. Figure 11 illustrates the process.

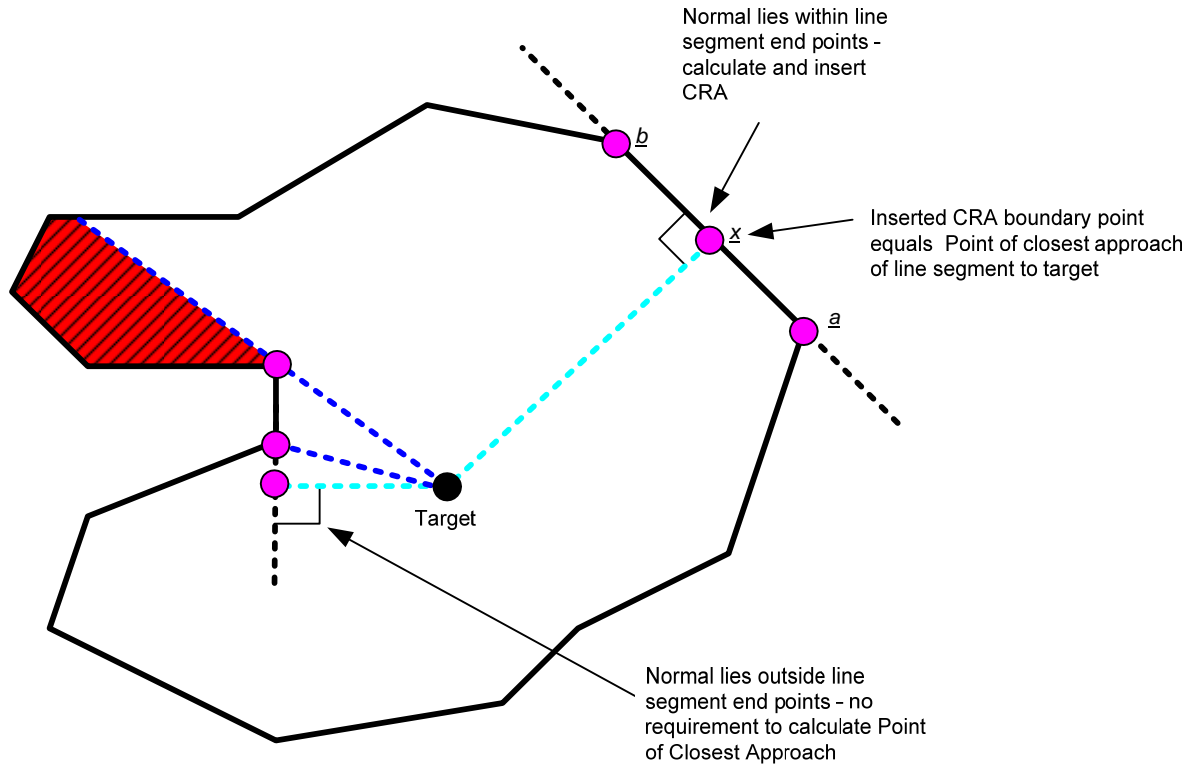


**Figure 11: Points of Closest Approach Condition**

We have already discussed the creation of a Terrain Profile Surface, and how terrain steps are defined in angular sectors centered on the target. The purpose of the terrain profile condition is to insert additional coordinates at the points of intersection between the line segments making up the CRA boundary and the terrain profile sector radials, so that the different analytical layers making up the overall clearance solution can be properly aligned geographically. Figure 12 illustrates the process.

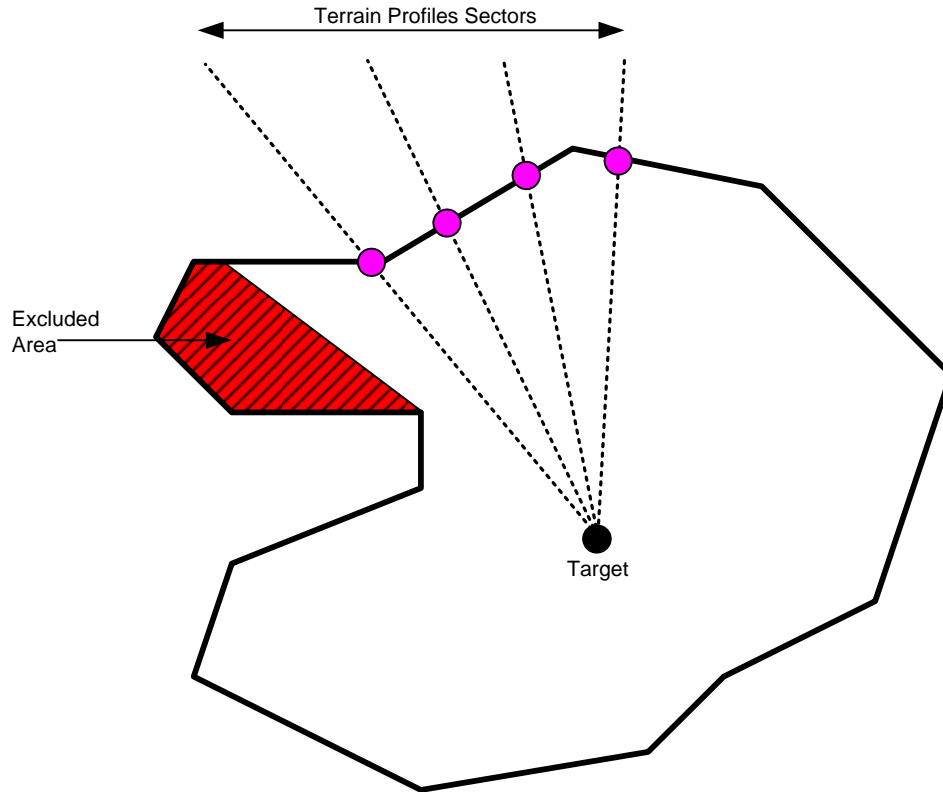


**Figure 12: Terrain Profile Condition**

For the CALCFAULT module, laser firing restrictions calculated for the fault/failure condition are partly driven by hazards posed to observers in populated Urban Areas outside the CRA. The urban area condition adds CRA boundary points that correspond to points of intersection between the boundary and radials from the target that bound each urban area in the vicinity of the Range.

The Urban Area bounding radials are defined by the ‘right-hand’ and ‘left-hand’ bearings ( $\theta_{MIN}$ ,  $\theta_{MAX}$ ) of the Urban Area limits with respect to the target, augmented by the fault/failure pointing error,  $\varepsilon$ . That is, the Urban Area bounding radials are defined by the bearings ( $\theta_{MIN} - \varepsilon, \theta_{MAX} + \varepsilon$ ). Figure 13 illustrates this process.

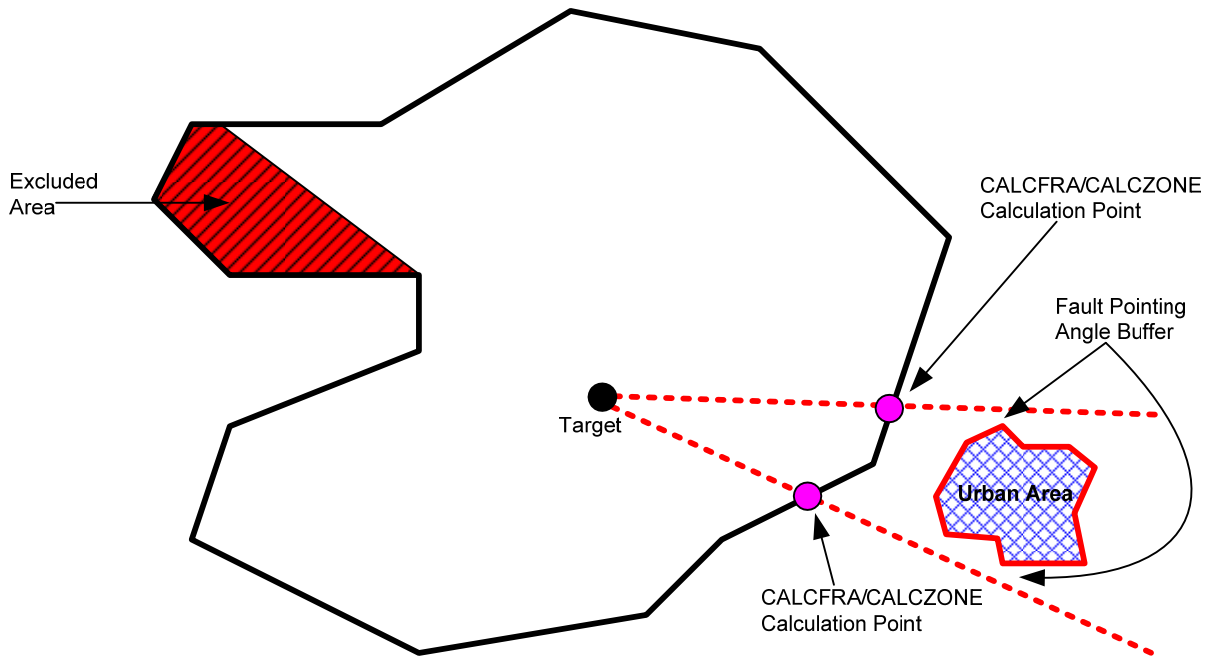


**Figure 13: Urban Area Condition**

The small increment condition ensures that the bearings of consecutive CRA boundary points differ by no more than 0.5 degrees. This smooths the calculation of the FFLFZ contours. Additional boundary points are added as required to ensure this. Figure 14 illustrates the process.

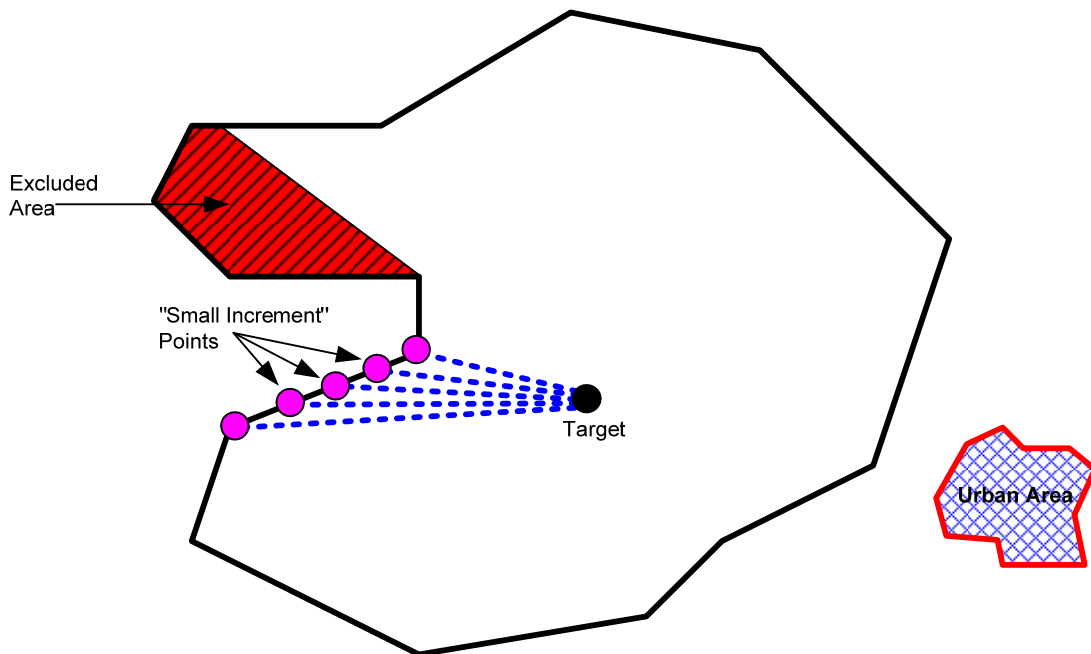


**Figure 14: Small Increment Condition**

As discussed in Section 2.7, CALCZONE defines the Fault-Free Laser Firing Zones (FFLFZ) based on the need to keep “undershoot” and “overshoot” laser pointing errors within the CRA, as shown in Fig. 5. Proper FFLFZ calculations require that each CRA boundary point corresponding to the maximum undershoot must be “mirrored” by a diametrically opposite boundary point, relative to the target, corresponding to the maximum overshoot. The undershoot/overshoot condition ensures that new boundary points are added to the CRA to satisfy this requirement, assuming such “mirror points” do not already exist. Figure 15 illustrates the process. Undershoot and overshoot restrictions, and their connection to the Terrain Profile Surface, are discussed in more detail in Section 3.5.

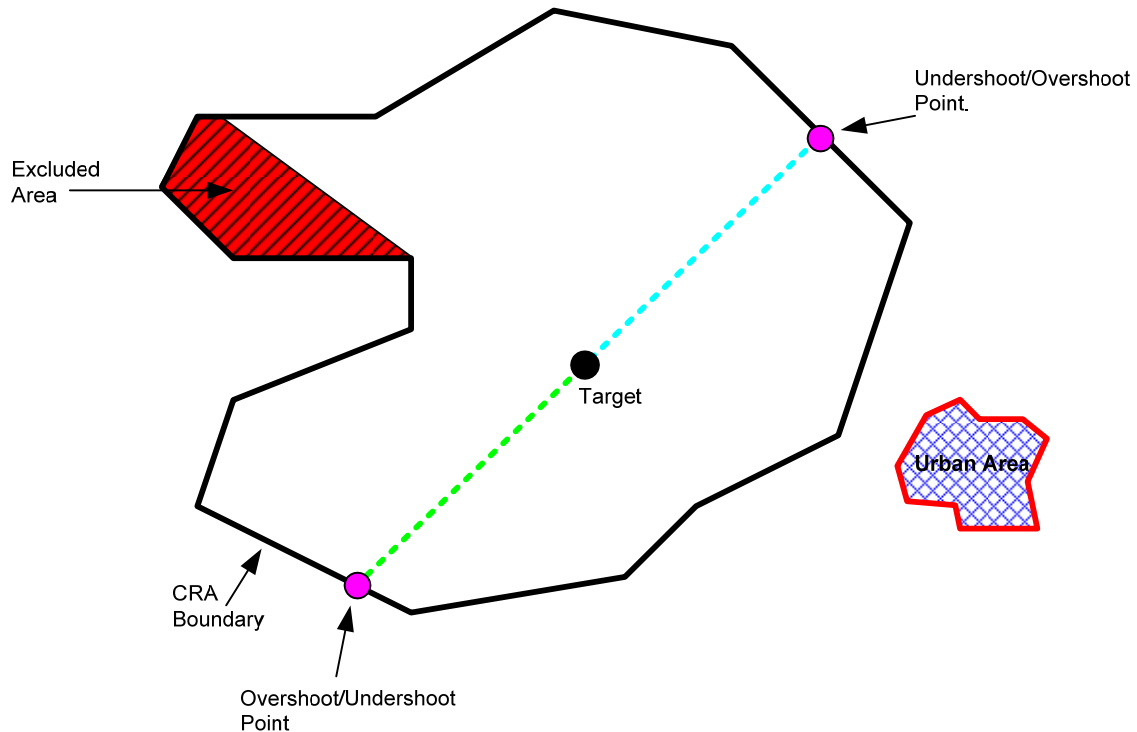


**Figure 15: Undershoot/Overshoot Condition**

After completion of the undershoot/overshoot step, a final check is made on the CRA boundary point list, as amended by the six RBPROG steps described above. The final check ensures that the point list is in sequential order, with respect to angular bearing to the target, and eliminates duplicate points. Collectively the six steps result in a set of CRA boundary coordinates that will be used subsequently by CALCZONE to calculate the permissible laser firing distances at various compass points around the target, i.e., the Fault-Free Laser Firing Zones. The final CRA for our sample case is shown in Fig. 16. The CRA boundary is in red and black, with the black line representing an alteration to the Range boundary needed to satisfy the star-shaped condition.



**Figure 16: RBPROG Analysis Result: CRA with Additional Boundary Points**

### 3.5 CALCZONE Analysis and Attack Track Definition

The second computational module, CALCZONE, performs the fault-free laser hazard analysis; i.e., it calculates the Fault-Free Laser Firing Zones (FFLFZ) for each designated aircraft altitude, and the specified target position, using the CRA defined in RBPROG. The general procedure for this has been previously described in Section 2.7. For any aircraft attack track, at any given altitude, the corresponding FFLFZ defines the maximum range-to-target at which the laser may be fired, assuming fault-free operation of the laser directional control system. The FFLFZ provide the analyst and Range personnel with a fault-free operating envelope, which ensures that laser energy will not go outside the CRA unless a fault/failure occurs.

We begin our description of CALCZONE analysis procedures by briefly reviewing the discussion of fault-free laser pointing errors, given in Section 2.3. We assume that the targeting system has a fault-free laser pointing error,  $\phi$ , with a corresponding fault-free laser pointing error distribution,  $f(\phi)$ . The maximum fault-free laser pointing error is  $\phi = \phi_{\max} = \alpha_{\max}$ . As defined in

Eq. 2.5, the value of  $\alpha_{\max}$  is calculated using the Threshold Probability for fault/failure,  $P_F$ , which is determined from the laser system hazard assessment and provided in the LSP. For any particular aircraft attack track, the fault-free laser pointing error could produce either an undershoot or an overshoot of the target.

As we recall from Section 2.7, defining the FFLFZ first requires calculation of the undershoot and overshoot ranges,  $R_u(\omega)$  and  $R_o(\omega)$ , corresponding to each possible aircraft altitude and to each radial,  $\omega$ , between the target and a CRA boundary point. These are the maximum ranges-to-target at which the laser can be fired, in order to keep to keep undershoot and overshoot laser pointing errors, respectively, within the CRA, as shown in Fig. 5. The overall maximum firing range,  $R(\omega)$ , is taken to be the smaller of the undershoot and overshoot ranges; that is,  $R(\omega) = \min\{R_u(\omega), R_o(\omega)\}$ . The FFLFZ for each aircraft altitude can then be defined as the set  $\{R(\omega) : \omega \in [0, 2\pi)\}$ , covering all possible radials to any boundary point.

We now consider the Target – Range Boundary geometry produced by both overshoot and undershoot of the target, due to the fault-free laser pointing error,  $\phi$ . We assume that the aircraft is flying a level attack track, at constant altitude or height  $H$ , and that the attack track is heading directly at the target, as shown in Fig. 5. The attack track thus lies within the vertical plane defined by the surface normal at the target, and the line connecting two “mirrored” CRA boundary points, such as those shown in Fig. 15. We designate the near and far boundary points as **BN** and **BF**, respectively. The range-to-target for an attacking aircraft can be defined in either of two ways: as a slant range along the laser-target vector, or as a ground range along a vector connecting the target to a point directly under the aircraft. In FFLFZ calculations we will use the ground range-to-target,  $R_0$ , measured along the curved earth surface.

Figure 17 shows the overshoot geometry for an Aircraft, **A**, at height  $H$ , with a (curved earth) ground range-to-target,  $R_0$ . We wish to ensure that the overshoot buffer angle (i.e., the angle between the aircraft-target and aircraft-**BF** vectors) is greater than or equal to the maximum fault-free laser pointing error. In this case, the laser energy will fall between the target, **T**, and the far boundary point, **BF**, i.e. within the CRA. As the aircraft approaches the target,  $R_0$  decreases, and the overshoot buffer angle increases. When the overshoot buffer angle is equal to the maximum fault-free laser pointing error,  $\phi = \alpha_{\max}$ , as shown in Fig. 17, then the aircraft ground range equals the overshoot range, i.e.,  $R_0 = R_o$ . Ground ranges smaller than the overshoot range give buffer angles larger than  $\alpha_{\max}$ , so if  $R_o$  is the maximum firing range, then any laser overshoots are safely contained within the CRA.

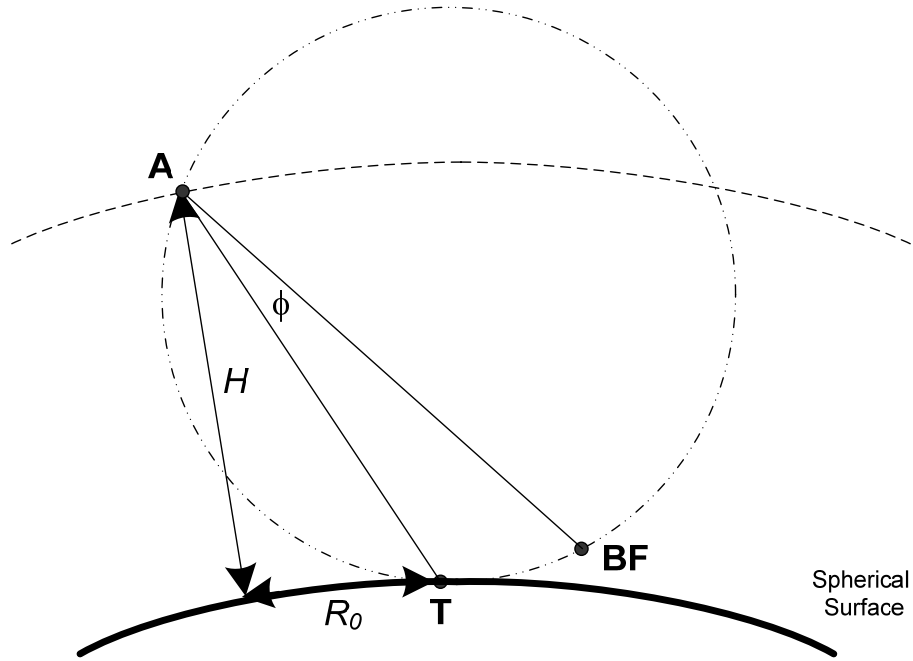


**Figure 17: Spherical Earth Target – Range Boundary Overshoot Geometry**

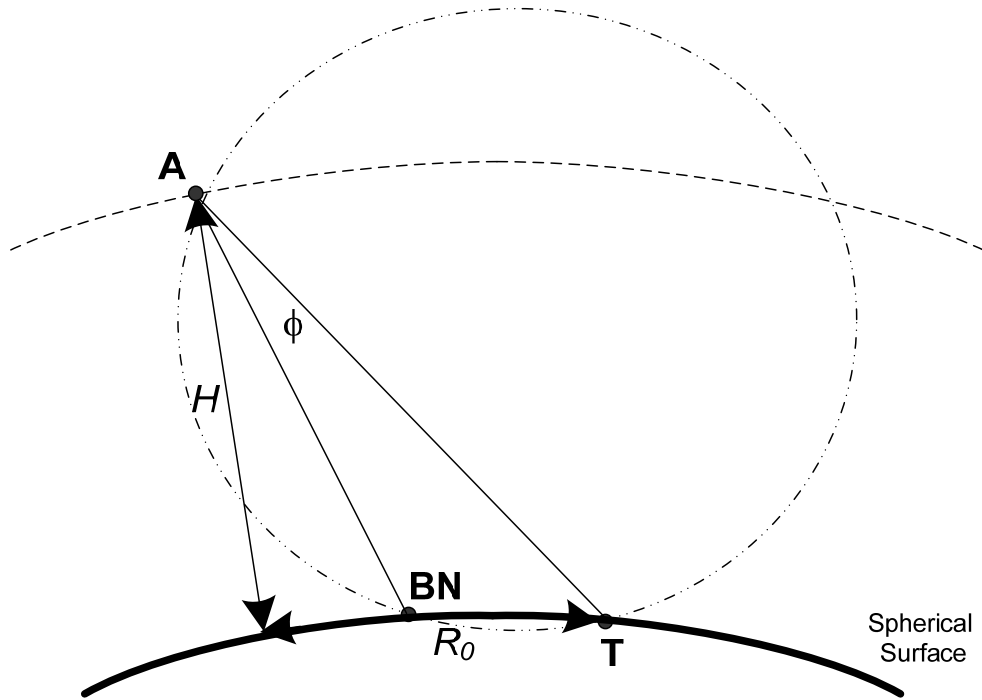


**Figure 18: Spherical Earth Target – Range Boundary Undershoot Geometry**

Figure 18 shows the undershoot geometry for the same Aircraft, constructed using the near boundary point, **BN**. In this case we wish to ensure that the undershoot buffer angle (i.e., the

angle between the aircraft-target and aircraft-**BN** vectors) is greater than or equal to than  $\alpha_{\max}$ . Once again, as the aircraft approaches the target,  $R_0$  decreases, and the buffer angle increases. When the undershoot buffer angle is equal to  $\alpha_{\max}$ , then the aircraft ground range equals the undershoot range, i.e.,  $R_0 = R_u$ .

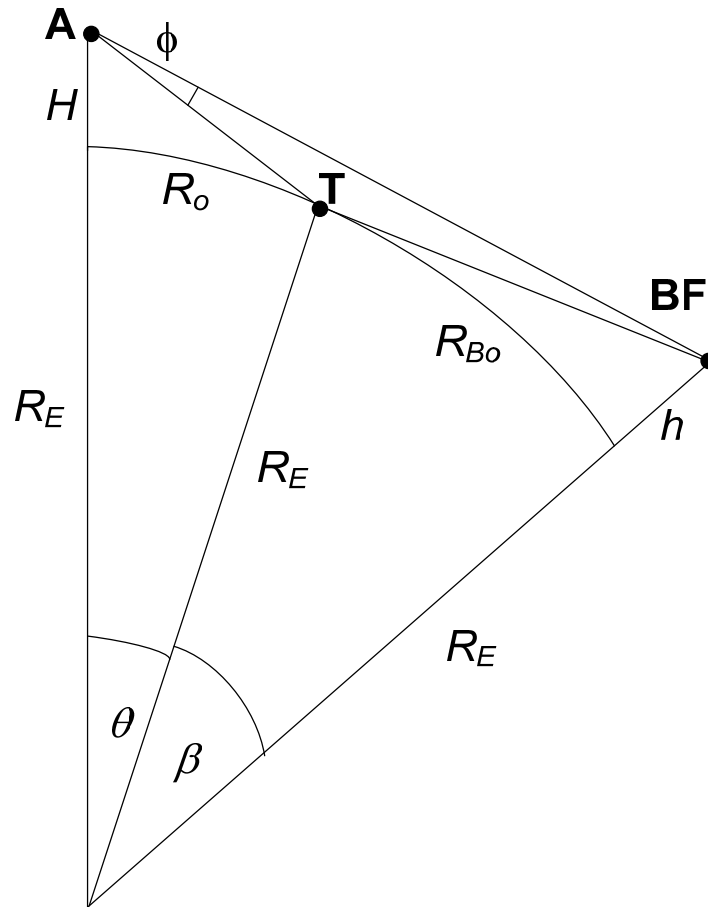


**Figure 19: Geocentric Overshoot Geometry and Parameters**

A set of equations allowing mathematical computation of the overshoot range [18] can be derived based on the Geocentric overshoot geometry and parameters shown in Fig. 19. In this Geocentric geometry, the point at the bottom represents the center of the Earth,  $R_E$  represents the radius of the Earth, and the curve once again represents the surface of the Earth. We should note that Fig. 19 represents the special case of the overshoot geometry where the overshoot buffer angle is  $\phi = \alpha_{\max}$  and the aircraft ground range is  $R_0 = R_u$ . Elevated terrain on the Range, and on the CRA boundary, is allowed for in the Figure. If we assume that the target is at sea level ( $h = 0$ ), then  $h = h_0$  is the elevation of the overshoot boundary point **BF**. For the elevated boundary point,  $R_{B0}$  represents the curved earth ground range from the target position to a zero elevation point directly beneath **BF**. Finally, if we assume that the radius of the Earth is large with respect to any ground range shown, then the two angles subtending the curved earth arc are small and

can be approximated by the corresponding ground range divided by  $R_E$ ; i.e.,  $\theta = R_o/R_E$  and  $\beta = R_{Bo}/R_E$ .

All the geometric parameters of Fig. 19 are known constants except for the (still undetermined) overshoot range  $R_o$  and the related angle  $\theta = R_o/R_E$ . Using the geometry of Fig. 19, we can derive a function relating  $\theta$  (and thus  $R_o$ ) to all the other parameters:

$$f_{\text{over}}(\theta) = a_1 \cos(\theta + \beta) + a_2 \cos \theta + \sqrt{(a_3 - \cos \theta)(a_4 - \cos(\theta + \beta))} - a_5 \quad (3.1)$$

where

$$\begin{aligned} a_1 &= \frac{R_E + h}{2\sqrt{R_E (R_E + h)} \cos \varphi_{\max}} \\ a_2 &= \frac{R_E}{2\sqrt{R_E (R_E + h)} \cos \varphi_{\max}} \\ a_3 &= \frac{R_E^2 + (R_E + H)^2}{2R_E (R_E + H)} \\ a_4 &= \frac{(R_E + h)^2 + (R_E + H)^2}{2(R_E + h)(R_E + H)} \\ a_5 &= \frac{R_E (R_E + h) \cos \beta + (R_E + H)^2}{2\sqrt{R_E (R_E + h)(R_E + H)^2} \cos \varphi_{\max}} \\ \beta &= \frac{R_{Bo}}{R_E} \end{aligned}$$

For  $\theta = R_o/R_E$ , we have  $f_{\text{over}}(\theta) = 0$ , and Eq. 3.1 becomes one equation in one unknown, which is (in theory) soluble for either  $\theta$  or  $R_o$ . In practice the equation is a very complex function of  $\theta$ , which does not have an analytical solution. Instead, it must be solved by iteration, evaluating the function for a series of estimated  $R_o$  values, and slowly closing in on the range for which Eq. 3.1 gives zero.

A similar equation for computation of the undershoot range can be derived based on the special case of the Geocentric undershoot geometry where the undershoot buffer angle is equal to  $\alpha_{\max}$ , the aircraft ground range equals the undershoot range,  $R_o = R_u$ , and  $\theta = R_u/R_E$ . The function relating  $\theta$  (and thus  $R_u$ ) to all the other parameters is now:

$$f_{\text{under}}(\theta) = a_1 \cos(\theta - \beta) + a_2 \cos \theta + \sqrt{(a_3 - \cos \theta)(a_4 - \cos(\theta - \beta))} - a_5 \quad (3.2)$$

Here the coefficients  $a_1$  through  $a_5$  have the same algebraic form as for Eq. 3.1 above, but in this case  $h = h_u$  is the elevation of the undershoot boundary point **BN**,  $\beta = R_{Bu}/R_E$ , and  $R_{Bu}$  represents the curved earth ground range from the target position to a zero elevation point

directly beneath **BN**. Just as for the overshoot calculation,  $f_{\text{under}}(\theta) = 0$  for  $\theta = R_u/R_E$ , and Eq. 3.2 reduces to one equation in one unknown, which can be solved for  $R_u$  by iteration.

We now return to the topic of elevated terrain surrounding the target, and the creation of a Terrain Profile Surface, one of the MATILDA set-up procedures discussed in Section 3.3. The Terrain Profile Surface provides the means of ensuring against the possibility of an undershoot beam accidentally irradiating elevated terrain areas outside the CRA, as shown in Fig. 20.

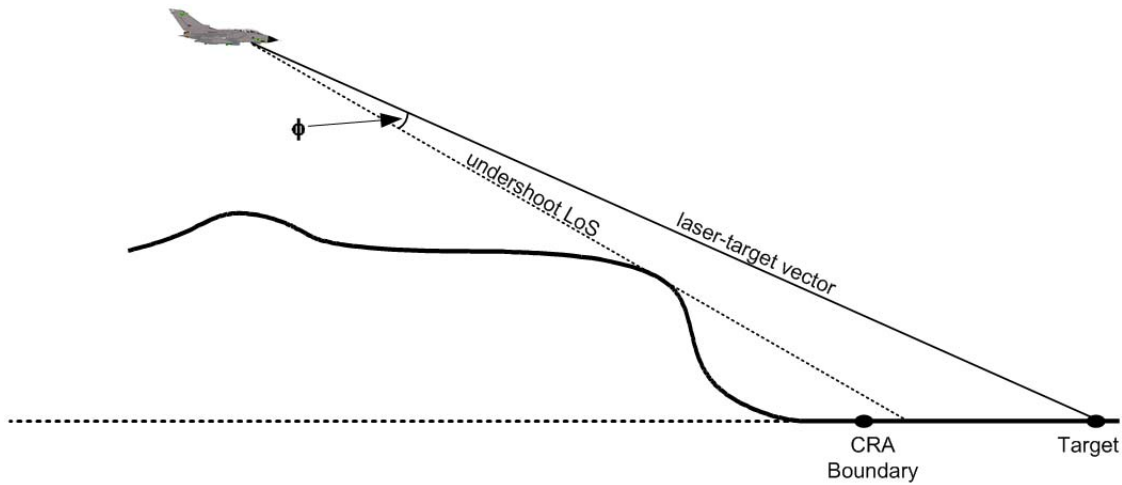


**Figure 20: Terrain Undershoot Problem**

The initial value computed for the undershoot range must be cross-checked against the terrain elevations given by the Terrain Profile Surface, in order to make sure that the initial undershoot range avoids this kind of off-Range irradiation problem. The procedure is to start with the near CRA boundary point and bring a line down from the zenith until it is tangent to the (stepped) Terrain Profile Surface. This point of contact is called the most prominent terrain step (MPTS). The tangent between **BN** and the MPTS is extended upwards to the aircraft height,  $H$ , creating a new aircraft-target slant range. The new ground range corresponding to this new slant range is now a second undershoot range that prevents irradiation of off-Range elevated terrain. The second value is compared to the initial result and the smaller of the two is the final undershoot range used to determine the FFLFZ.

Once we have calculated the undershoot and overshoot ranges,  $R_u(\omega)$  and  $R_o(\omega)$ , corresponding to aircraft height,  $H$ , and to some radial angle,  $\omega$ , between the target and the near CRA boundary point, the overall maximum firing range,  $R(\omega)$ , is taken to be the smaller of the two. The FFLFZ for that height can then be defined by calculating the set  $\{R(\omega): \omega \in [0, 2\pi)\}$ , covering all possible radials to any boundary point. The FFLFZ is typically plotted by laying down each range at the proper radial angle on the map, plotting the end point of each range vector, and then connecting all the end points to make a closed contour about the target. This process is repeated for each proposed attack height. The nested series of contours produced defines a three-dimensional envelope for the acceptably-safe firing of the laser during fault-free operation of the

laser directional control system. An example of the FFLFZ contour set, generated by MATILDA for our Tain Range sample case, is shown in Fig. 21.

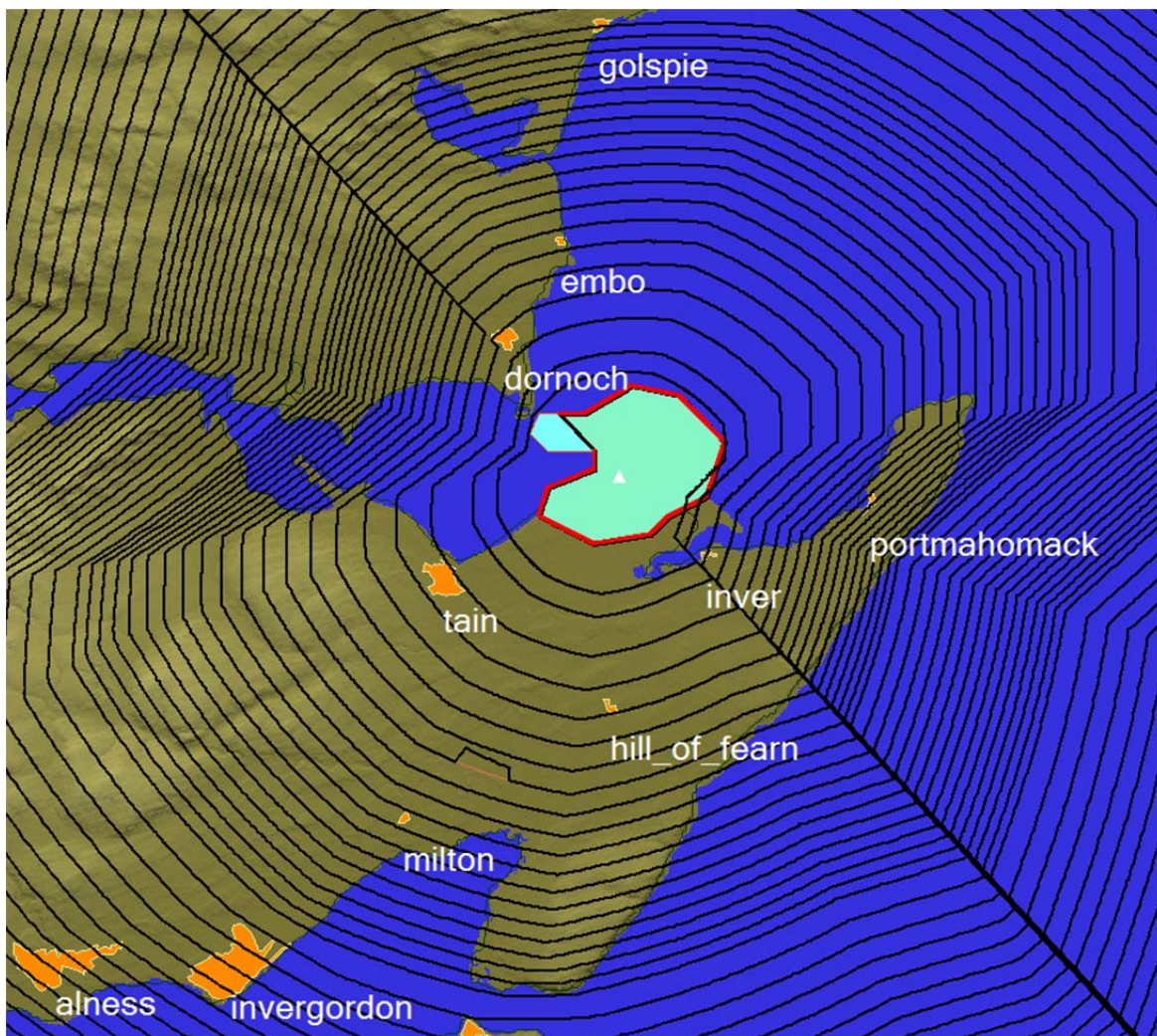


**Figure 21: MATILDA Generated Fault-Free Laser Firing Zones**

Generation of the FFLFZ contours completes the fault-free laser hazard analysis and lays the foundation for the probabilistic fault/failure hazard analysis performed in CALCFAULT. Prior to execution of CALCFAULT; however, a specific laser attack scenario must be defined. MATILDA provides a feature, the Attack Track Waypoint Editor that allows an analyst to overlay an attack track, defined by a series of waypoints, onto the map. The data entry for waypoints includes waypoint coordinates, aircraft altitude, aircraft velocity, and whether the laser is firing at that waypoint. With this data, MATILDA compares the proposed attack track against the altitude limitations defined by the FFLFZ and indicates to the analyst those portions of the track that are cleared for laser firing and those where laser firing is prohibited. Fig. 22 gives an example of such a user-entered attack track. Note that the vast majority of the attack

track is colored green, and hence cleared for firing, but a small portion at the end violates FFLFZ altitude limitations, and is therefore colored red. Only the portion of the attack track that clears FFLFZ restrictions is analysed during CALCFAULT execution.

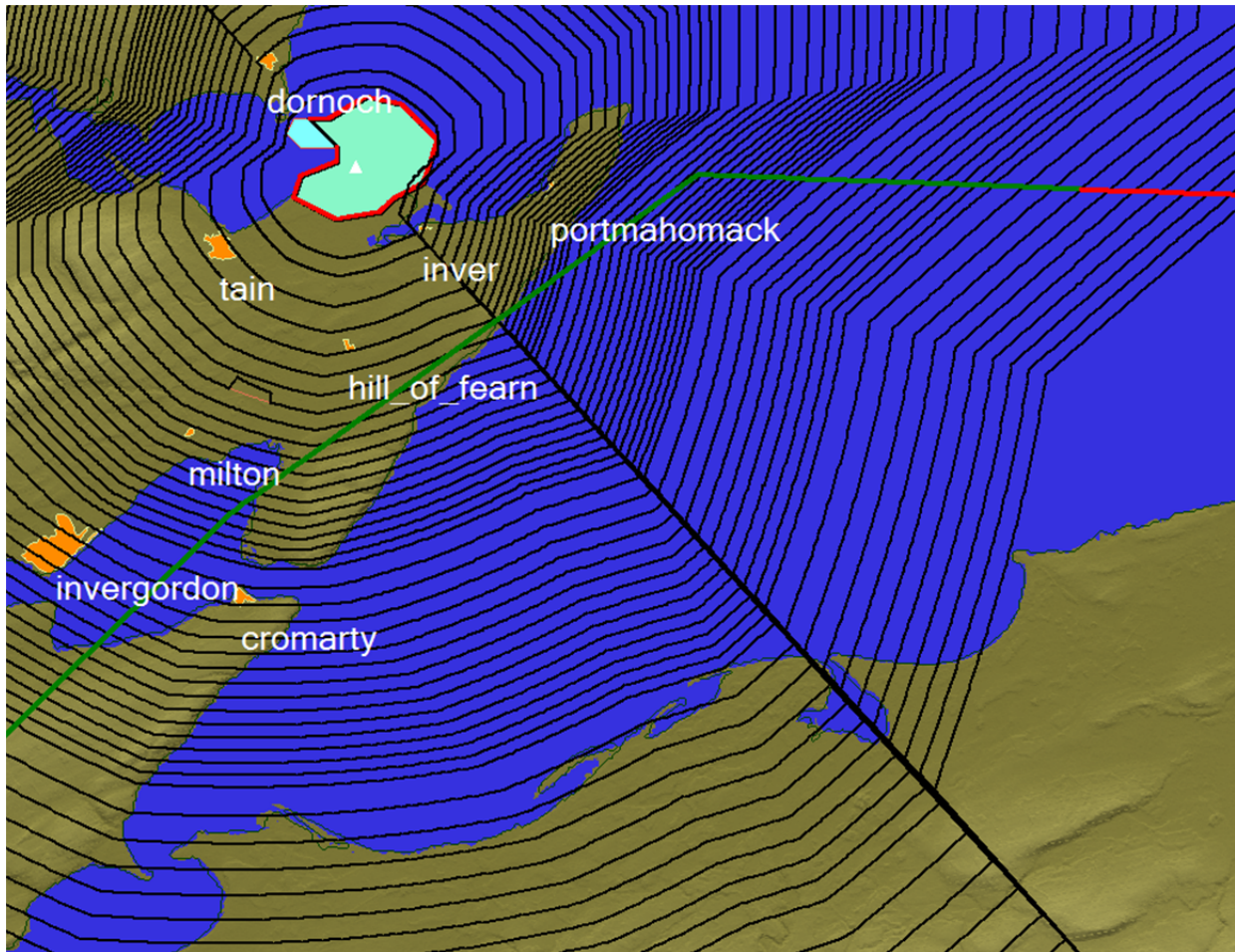


Figure 22: Fault-Free Attack Track Check

### 3.6 CALCFAULT Analysis

The third module, CALCFAULT, performs the probabilistic fault/failure hazard analysis for the designated and cleared laser attack scenario, to determine if any additional restrictions must be imposed on the laser firing envelope permitted by the FFLFZ. The CALCFAULT analysis quantifies the actual risk for firing along the designated attack track, in the event of a fault in, or a failure of, the laser directional control system. The probabilistic Expectation Model discussed in Section 2.5 is used in this analysis. Key input parameters for the CALCFAULT analysis include laser system parameters, attack track data, population densities of the Urban Areas surrounding the Range, the terrain computational grid (points on the ground for which ocular damage probability is computed), and of course, the maximum acceptable value of the overall expectation value,  $E_{MOVLMAX}$ .

Since a fault/failure could occur at any point during the course of the cleared laser attack scenario, a large number of failure cases, each representing a possible failure at a different point along the attack track, must potentially be evaluated and their overall expectation values compared to  $E_{\text{MOVLMAX}}$ , in order to complete the fault hazard analysis. Generally, the number of failure cases evaluated is equal to the number of pulses,  $N_p$ , fired during the attack scenario; i.e., the fault hazard analysis is performed for a possible failure at each of the laser firing positions. For each laser pulse emitted after the fault/failure, the CALCFAULT algorithm evaluates a corresponding expectation value,  $e_{\text{MOVL}}$ , that a MOVL will occur in the unprotected population surrounding the CRA. The number of pulses emitted after a fault or failure has occurred depends on the pulse repetition frequency (PRF) and the length of time required for the laser to cease firing. Consequently, the overall expectation value,  $E_{\text{MOVL}}$ , for a particular failure case, is the sum of the individual pulse  $e_{\text{MOVL}}$  values for the period of time during which the laser continues to fire.

The overall expectation value,  $E_{\text{MOVL}}(i)$ , of an unprotected observer sustaining a MOVL as a result of a Fault or Failure occurring on the  $i$ -th pulse emitted during laser firing operations is given by [18]:

$$E_{\text{MOVL}}(i) = P_F \sum_{j=0}^{m-1} e_{\text{MOVL}}(i+j) \quad (3.3)$$

where  $P_F$  is the probability of a fault occurring on the  $i$ -th pulse,  $m$  is the maximum number of pulses emitted during a fault, and  $e_{\text{MOVL}}(i)$  is the expectation value of an unprotected observer sustaining a MOVL as a result of the  $i$ -th pulse. The latter is given by the expression:

$$e_{\text{MOVL}}(i) = \int_{\theta} \int_{\phi} f(\theta, \phi) g(\theta, \phi) d\theta d\phi \quad (3.4)$$

In Eq. 3.4,  $f(\theta, \phi)$  is the PDF representing the (fault) laser pointing error and will depend on the laser sightline control system. The random variables  $\phi \in \Phi$  and  $\theta \in \Theta$  represent a radial pointing error from the laser–target vector and a ‘compass’ direction for the radial error respectively. The quantity  $g(\theta, \phi)$  is a real-valued function representing the expected number of people in the beam footprint sustaining a MOVL, and which is estimated by

$$g(\theta, \phi) = \rho(\theta, \phi) S_e(\theta, \phi) Q \left[ w_{\text{MOVL}} \left( h(r(\theta, \phi)) \right) \right] \quad (3.5)$$

Here  $\rho(\theta, \phi)$  is the local population density in the direction  $(\theta, \phi)$ ,  $S_e$  is the area of the beam footprint on the ground in the direction  $(\theta, \phi)$ , and  $Q \left[ w_{\text{MOVL}} \left( h(r(\theta, \phi)) \right) \right]$  is the probability of ocular damage from laser energy density,  $h$ , at laser–observer distance,  $r$ , in the direction  $(\theta, \phi)$ . The quantity  $Q[x]$  is the upper tail of the cumulative normal distribution,

$$Q[x] = \frac{1}{\sqrt{2\pi}} \int_x^{\infty} e^{-\frac{t^2}{2}} dt \quad (3.6)$$

and represents the *probability* that a person who has an ocular exposure, produced by a laser pulse emitted in the direction  $(\theta, \phi)$ , receives a MOVL. The lower limit  $x = w_{\text{MOVL}}(h(r(\theta, \phi)))$  is given by

$$w_{\text{MOVL}}(h(r(\theta, \phi))) = \frac{a \left( -\log_e (h(r(\theta, \phi))) + \frac{\eta^2}{2} \right) + b(d)}{\sqrt{1 + a^2 \eta^2}} \quad (3.7)$$

where:

$h(r(\theta, \phi))$  = the laser energy density at the cornea, distance  $r$  in the direction  $(\theta, \phi)$  in  $\text{mJm}^{-2}$

$$a = 1.715$$

$$b(d) = 8.5169 + 3.73538 \log_{10} d = \begin{cases} 14.035 & (G_m = 1) \\ 15.820 & (G_m > 1) \end{cases}$$

$d$  = the diameter of the laser image on the retina

$$= \begin{cases} 30 \mu\text{m} & \text{for unaided (naked-eye) viewing } (G_m = 1) \\ 90 \mu\text{m} & \text{for aided viewing with magnifying optics } (G_m > 1) \end{cases}$$

$\eta$  = standard deviation of log-irradiance

$$= 1.1$$

Each direction  $(\theta, \phi)$  will also have an associated range,  $r$ , between the aircraft and the intersected ground point, which is also the range between the laser and a possible observer. This, along with the laser beam  $1/e$ -pt beam divergence,  $\phi_e$ , is required to calculate a beam area, or beam footprint,  $S_e$ , produced when the beam intersects the ground. Then, using the population density,  $\rho(\theta, \phi)$ , associated with this beam area, we may calculate the expected number of people,  $N$ , exposed within the beam footprint:

$$N = \rho S_e \quad (3.8)$$

We now turn to a discussion of the computational methods used to numerically evaluate the Expectation Model described above.

The integral in Eq. 3.4 gives the expectation value of an unprotected observer sustaining a MOVL as a result of a single pulse emitted after a fault/failure event. Since it is generally not feasible to obtain an analytic form for  $g(\theta, \phi)$ , this integral cannot be evaluated analytically. Instead, the CALCFAULT algorithm numerically evaluates  $e_{\text{MOVL}}(i)$ , using a set of terrain computational points representing the region around the target that *could be* irradiated while the

laser is still firing following a directional control system fault or failure. The elemental probability that any given terrain computation point within this region is irradiated can be evaluated using the fault pointing error probability density function,  $f(\theta, \phi)$ . The expected number,  $g(\theta, \phi)$ , of observers sustaining a MOVL at each of the computational terrain points is estimated as the product of the ground-projected beam area (the beam “footprint”) with the local population density value at that point.

Eq. 3.4 can thus be evaluated *numerically* as the *weighted* sum of the expectation values for  $n$  terrain points, which correspond to the ground intersection points of a set of laser pointing error directional vectors  $(\theta, \phi)$ , so that

$$e(i)_{MOVL} = \sum_{i=1}^n we(\theta_i, \phi_i) \times f(\theta_i, \phi_i) \times g(\theta_i, \phi_i) \quad (3.9)$$

Here the expectation value sum over the  $n$  terrain points is expressed in terms of the directional vectors  $(\theta, \phi)$  that point to them. For a flat-earth geometry, however, it is most convenient to evaluate the expectation value sum over a Cartesian grid of equally spaced ground points  $(x, y)$ . For each Cartesian ground point,  $(x_i, y_i)$ , we can compute the angles,  $\theta_i$  and  $\phi_i$ , representing the corresponding directional vector:  $\theta_i = \text{function1}(x_i, y_i)$  and  $\phi_i = \text{function2}(x_i, y_i)$ . The sample weighting function,  $we(\theta_i, \phi_i)$ , is then related to the determinant of the Jacobian matrix used to transform the PDF of the laser pointing error directional vectors from angle space to ground space.

To summarize, numerical evaluation of the single pulse expectation value in Eq. 3.9 consists of the following sequence of steps. First, we set up a Cartesian pointing error grid in the ground plane that covers the range of directions in which laser energy could be fired before laser firing is inhibited. Next, for each of the  $n$  grid points we calculate the angles  $\theta_i$  and  $\phi_i$ , and determine the size of the (ground-projected) laser beam footprint. Finally, we calculate the appropriate values of  $g(\theta_i, \phi_i)$  and  $f(\theta_i, \phi_i)$  at each point and evaluate the weighted sum.

This process is repeated for each of the  $m$  pulses fired following a fault/failure event. The overall expectation value for this fault/failure event, given by Eq. 3.3, is then the sum of the  $m$  single pulse expectation values, multiplied by the probability that the fault failure will occur. As mentioned, CALCFAULT will calculate  $N_p$  overall expectation values during the fault hazard analysis, one for a possible failure at each of the  $N_p$  laser firing positions along the cleared laser attack track. If any of these values exceed the maximum acceptable value,  $E_{MOVLMAX}$ , then firing is prohibited over that portion of the attack track.

To conclude Section 3.6, we now give CALCFAULT results for our Tain Range sample case. For the sample case, MATILDA first uses the 20 Hz PRF, and the FFLFZ-cleared attack track shown in Fig. 22, to determine the location of each pulse emitted during the attack. This gives 5200 possible laser firing positions. For each firing position CALCFAULT determines a beam footprint whose boundaries are defined by the maximum (fault) pointing error entered (20 degrees). As mentioned, the only terrain grid points that need be evaluated for each pulse, and

corresponding  $e_{\text{MOVL}}$ , are those that fall within the range of directions in which laser energy can be directed before laser firing is inhibited.

In this sample case each  $E_{\text{MOVL}}$  value, evaluated for a fault at one of the 5200 possible laser firing positions, consists of the sum of 60  $e_{\text{MOVL}}$  values, representing the 60 pulses fired during the 3 second laser shutdown period following the fault. Fig. 23 shows a comparison of all 5200  $E_{\text{MOVL}}$  values to the acceptable risk threshold. For the UK Tain Range case shown here, the standard UK value of  $E_{\text{MOVLMAX}} = 10^{-8}$  was used. As we see, the FFLFZ-cleared attack track for the Tain Range case does not exceed the acceptable risk threshold for a laser control error at any of the 5200 firing points. It would therefore be approved for laser firing without modification.

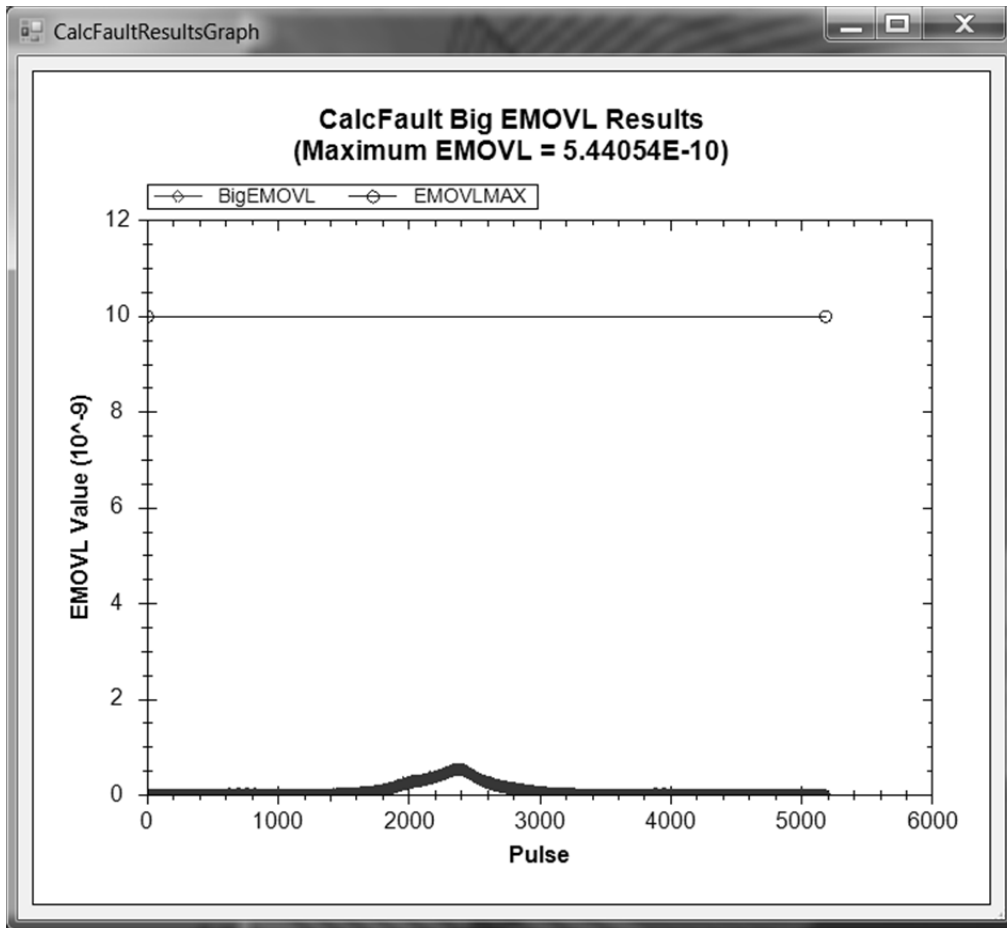


**Figure 23: Comparison of EMOVL Values to the EMOVLMAX Criterion**

## 4 DISCUSSION

The concept of PRA and its application to military laser safety in outdoor environments has been gaining in ascendancy in recent years, as the advantage of, and the necessity for, a probabilistic approach to laser hazard analysis has become increasingly accepted. The advantage of a PRA-based solution over the standard risk analysis method involving evaluation of the NOHD is amply illustrated in Fig. 24, in which a Deterministic Ocular Hazard Zone (DOHZ), based on the single pulse NOHD, is compared with a probabilistically derived Laser Hazard Area Trace (LHAT) that has been defined for all laser pulses emitted during the attack sequence. In this case, the PRA-based LHAT is much smaller in extent than the DOHZ. Additionally, the variation of risk with location inside the LHAT can be evaluated, whereas the interior of the DOHZ can only be described as ‘unsafe’. As an example of how this might benefit the DOD, AFRL personnel have done probability of injury analysis, as a function of location of ground observers, for reflections from airborne ordnance targeted by Army ground-based laser systems.

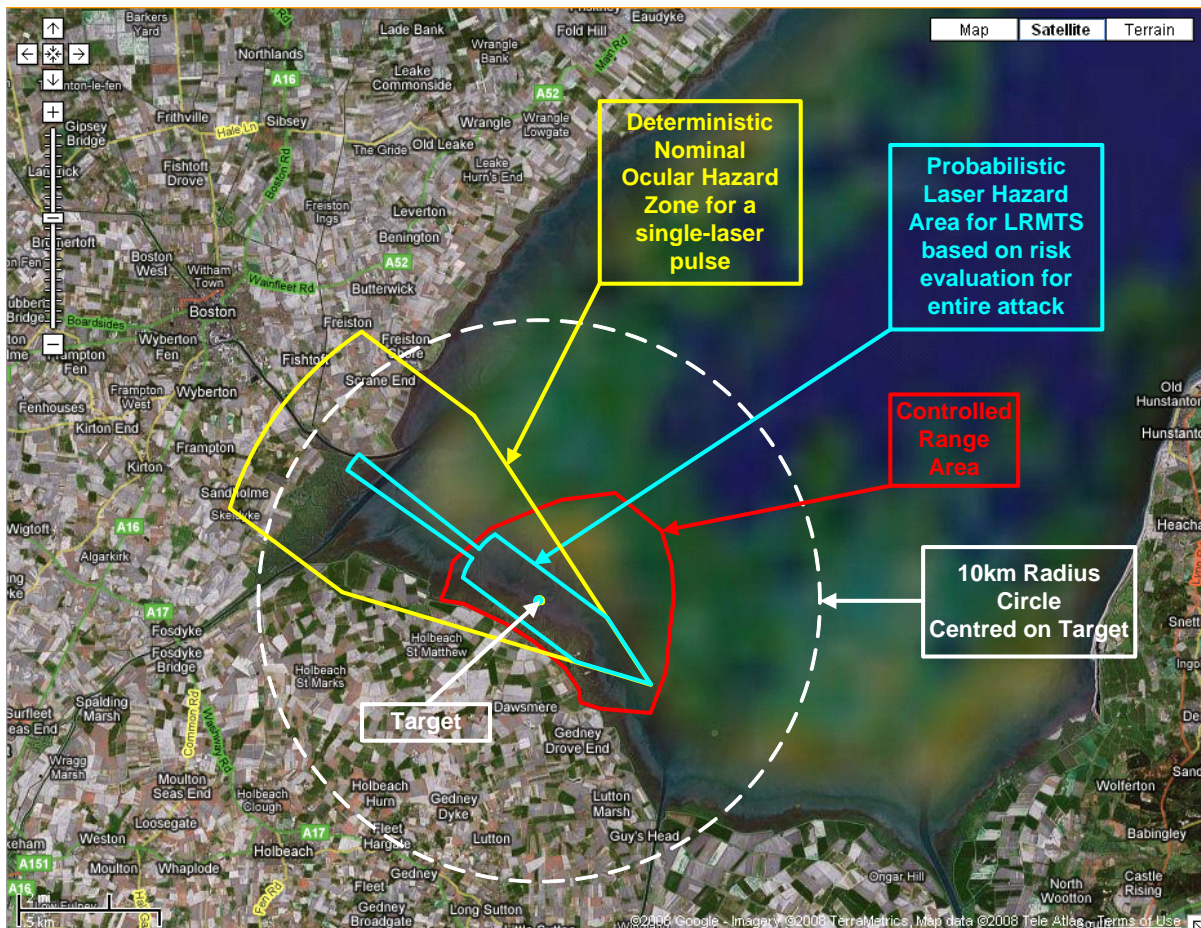


**Figure 24: Comparison of a PRA-Based Laser Hazard Area Trace with a Deterministic Ocular Hazard Zone**

PRA-based methods are thus perceived to offer greater flexibility to the laser system operator, while maintaining acceptable levels of safety for unprotected members of the general public. On the other hand, the PRA-based method does not come without additional cost. Due to the smaller margins of safety involved in the PRA method, based on what is deemed to satisfy the ALARP principle, a substantial amount of preliminary effort is required to establish the performance attributes of the laser system and ensure the validity of the subsequent hazard analysis. The Laser System Safety Investigation (LSSI), needed to adequately characterise the fault-free performance and fault/failure characteristics of the laser directional control system, has been described in detail in a previous publication [14].

Perhaps the most important requirement of the PRA-based clearance method is the determination of what level of risk is deemed to be acceptable to unprotected members of the general public in the vicinity of laser system test or training operations. The acceptable level of risk will vary from one jurisdiction to another, and should be decided at an appropriate policy level within the host country's chain of executive responsibility. As mentioned previously, the maximum acceptable risk level set by the UK MOD is  $10^{-8}$  occurrences of MOVL per attack. There is currently no acceptable risk level specified for US Ranges, because PRA is still too new in DOD applications. The identified acceptable level of risk will have an impact on the flexibility of the resulting clearance restrictions. In general, the more stringent are the safety criteria, the less flexible will be the resulting clearance restrictions.

## 5 CONCLUSIONS

The use of Probabilistic Risk Assessment (PRA) techniques to perform laser safety and hazard analysis for high output lasers in outdoor environments has become an increasingly accepted alternative to standard risk analysis methods, based on Maximum Permissible Exposure (MPE) limits. Over the past ten years, the United Kingdom (UK) Ministry of Defence (MoD) and the United States (US) Air Force Research Laboratory (AFRL) have collaborated to develop a jointly-owned, PRA-based, laser Range safety tool, the Military Advanced Technology Integrated Laser hazard Assessment (MATILDA) system.

PRA-based laser hazard analysis offers a number of advantages over standard risk analysis methods. First, it provides a quantified assessment of human risk (probability of injury) as a function of location. Second, it captures the probabilities and consequences of human error and laser fault/failure conditions, factors which are critical to valid hazard assessments for military laser operations in uncontrolled outdoor environments. Third, and most importantly, PRA analysis does not assume, or require, a zero risk condition as a final result. Instead, it compares the quantified risk against a maximum acceptable (non-zero) risk value. This produces less restrictive Range clearances, while still maintaining safety levels deemed acceptable for Range personnel and members of the public. This last advantage is critical for the UK, where the small size of UK Ranges and the possibility that laser beams might escape Range boundaries make a zero risk condition for Range testing unacceptably restrictive.

Over the past four decades, the UK MoD has pioneered the development of PRA-based models for laser hazard assessment, using them to assess laser irradiation risks to unprotected persons

from outdoor test and training operations on UK military Ranges. The United States Air Force (USAF) has also identified the need for a PRA-based approach in the quantification of laser hazards. Discussions between the USAF and the UK MoD revealed a common objective in developing a jointly owned, PRA-based, laser Range safety tool. Thus, UK laser PRA modelling expertise and AFRL expertise in development of advanced laser hazard assessment tools were combined to create the MATILDA tool.

The MATILDA system is a new software tool based on open-source Geographic Information System (GIS) technology, which integrates relevant laser system performance parameters with environmental data appropriate to the Range location where the system is being operated. It provides a modern, low-cost, portable computational environment, which may be tailored equally to the needs of the local Range safety technician and the expert analyst. MATILDA provides the user/analyst with the means to efficiently assess risks arising from different attack profiles on any given target, and ensures that the results are consistent with acceptable safety criteria. The result is an optimum level of flexibility in laser Range operations, while still maintaining high standards of safety for unprotected persons near the Range. MATILDA is the first military software tool to contain a complete end-to-end laser PRA model, crafted for Range applications, and with generalized terrain modelling. In the future it will provide a starting point for development of more advanced laser PRA models and tools.

## 6 REFERENCES

1. Bedford, T. and Cooke, R. M., *Probabilistic Risk Analysis: Foundations and Methods*, Cambridge University Press, Cambridge, UK (2001).
2. Kummamoto, H. and Henley, E. J., *Probabilistic Risk Assessment and Management for Engineers and Scientists (Second Ed.)*, Institute of Electrical and Electronic Engineers, Inc., New York, NY (1996).
3. Smith, P. A., *J. Laser Appl.* **6**, 101 (1994).
4. Sliney, D. H., *Optics and Laser Tech.* **27**, 279 (1995).
5. Gardner, R. and Smith, P. A., *Optics and Laser Tech.* **27**, 15 (1995).
6. Smith, P. A., Van Veldhuizen, D. A. and Polhamus, G. D., "High-Energy Laser Systems: Analytical Risk Assessment and Probability Density Functions," *Proceedings of the SPIE* **4246**, 145 (2001).
7. *MIL-HDBK-828A: Laser Safety on Ranges and in Other Outdoor Areas*, DOD Handbook, Department of Defense, Washington, DC (1996).
8. American National Standards Institute, *ANSI Standard Z136.1-2007: American National Standard for Safe Use of Lasers*, Laser Institute of America, Orlando, Florida (2007).
9. International Electrotechnical Commission, *IEC 60825-1-2007: Safety of Laser Products, Part 1 – Equipment Classification and Requirements*, Geneva, Switzerland (2007).
10. Kennedy, P. K., Huantes, D. F., Thomas, R. J., Smith, P. A., Riley, T. and Flemming, B. K., "US/UK Collaboration on PRA Models for Military Laser Safety Analysis," *Proceedings of the International Laser Safety Conference* **7**, 228 (2005).
11. Huantes, D. F., Kennedy, P. K., Thomas, R. J., Mastro, P. C., Mitchell, W., Keppler, K. S. and Menninger, M., "Laser Range Management Software (LRMS) and PRA Concept Demonstrator," *Proceedings of the International Laser Safety Conference* **7**, 232 (2005).
12. Flemming, B. K., "MATILDA: A Joint UK/US Military Laser Range Clearance Utility Based on Probabilistic Hazard Assessment Techniques," *Proceedings of the International Laser Safety Conference* **9**, 362 (2009).
13. Flemming, B. K., Huantes, D. F. and Kennedy, P. K., "MATILDA: A Laser Range Hazard Assessment Utility," *Proceedings of the International Laser Safety Conference* **10**, 239 (2011).

14. Flemming, B. K., Grieve, L. M., Huantes, D. F., Kennedy, P. K. and Flower, M. D., "Laser System Safety Investigations for PRA Model Development," *Proceedings of the International Laser Safety Conference* **11**, 118 (2013).
15. *JSP 390, Military Laser Safety: Volume 2 – Laser Safety Management System (2012 Edition)*, UK Ministry of Defence, London, UK (2012).
16. *Health and Safety at Work Act 1974 (c. 37)*, Her Majesty's Stationary Office, London, UK (1974).
17. Covello, V.T. and Merkhofer, M.W., *Risk Assessment Methods: Approaches for Assessing Health and Environmental Risks*, Plenum Press, New York, NY (1993).
18. Devoy, D., Flemming, B., and Harding, S., *Handbook for Laser Probabilistic Risk Assessment*, SELEX Galileo Technical Report: AP50053679, SELEX Galileo, Edinburgh, UK (2012).
19. Ahmed, E., Early, E., Huantes, D., Thomas, R. and Wooddell, D., "A Probabilistic 1064 nm Dose Response Model Version-1.0," DOD Technical Report No. AFRL-RH-BR-TR-2009-0021, U. S. Air Force Research Laboratory, Brooks City-Base, TX (2009).
20. Polhamus, D. G. and Smith, P. A., "A Probabilistic Model of 1315 nm Laser Bioeffects," DOD Technical Report No. AFRL-HE-BR-TR-2004-0143, U. S. Air Force Research Laboratory, Brooks City-Base, TX (2004).